PERFORMANCE IMPROVEMENT FOR SITUATIONAL AWARENESS AND RESTORATION OF DISTRIBUTION SYSTEMS

A THESIS SUBMITTED TO
THE GRADUATE SCHOOL OF NATURAL AND APPLIED SCIENCES
OF
MIDDLE EAST TECHNICAL UNIVERSITY

BY

UĞUR CAN YILMAZ

IN PARTIAL FULFILLMENT OF THE REQUIREMENTS
FOR
THE DEGREE OF MASTER OF SCIENCE
IN
ELECTRICAL AND ELECTRONIC ENGINEERING

JUNE 2021

Approval of the thesis:

PERFORMANCE IMPROVEMENT FOR SITUATIONAL AWARENESS AND RESTORATION OF DISTRIBUTION SYSTEMS

submitted by **UĞUR CAN YILMAZ** in partial fulfillment of the requirements for the degree of **Master of Science** i**n Electrical and Electronic Engineering, Middle East Technical University** by,

Prof. Dr. Halil Kalıpçılar
Dean, Graduate School of **Natural and Applied Sciences** _____

Prof. Dr. İlkay Ulusoy
Head of the Department, **Electrical – Electronics Engineering** _____

Assoc. Prof. Dr. Murat Göl
Supervisor, **Electrical – Electronics Engineering, METU** _____

Examining Committee Members:

Prof. Dr. Ali Nezih Güven
Electrical – Electronics Engineering, METU _____

Assoc. Prof. Dr. Murat Göl
Electrical – Electronics Engineering, METU _____

Prof. Dr. Umut Orguner
Electrical – Electronics Engineering, METU _____

Prof. Dr. Saffet Ayasun
Electrical – Electronics Engineering, Gazi University _____

Asst. Prof. Dr. Oğuzhan Ceylan
Electrical – Electronics Engineering, Kadir Has University _____

Date: 30.06.2021

I hereby declare that all information in this document has been obtained and presented in accordance with academic rules and ethical conduct. I also declare that, as required by these rules and conduct, I have fully cited and referenced all material and results that are not original to this work.

Name Last name : Uğur Can Yılmaz

Signature :

ABSTRACT

PERFORMANCE IMPROVEMENT FOR SITUATIONAL AWARENESS AND RESTORATION OF DISTRIBUTION SYSTEMS

Yılmaz, Uğur Can
Master of Science, Electrical and Electronic Engineering
Supervisor: Assoc. Prof. Murat Göl

June 2021, 84 pages

Electricity has a crucial role in modern life, and its absence may cause catastrophic complications. Restoration of distribution systems requires an efficient decision support mechanism as well as an accurate real-time operation. Considering the utmost importance of fast restoration of the distribution system to provide uninterrupted electricity, a decision support mechanism is required to employ an efficient analysis of the system. Therefore, it is crucial to analyze the system in a fast manner. This thesis presents a computationally efficient partitioning method using a novel numeric algorithm to detect the ring structure in order to conduct the required analyses in a fast manner. Moreover, to improve the situational awareness during the restoration, a situational awareness tool is developed. The tool uses received measurements from the energized sections to estimate the observable states and to update unreliable load/generation forecasts/profiles. The proposed tool employs three-phase Least Absolute Values (LAV) estimator with a linearized measurement function to improve the computational performance without loss of accuracy significantly. Finally, the proposed situational awareness tool uses an efficient power flow formulation based on the well-known forward/backward sweep algorithm to detect any infeasible restoration strategy.

Keywords: Distribution System Restoration, Three-Phase State Estimation, Situational Awareness Tool, Forward/Backward Power Flow, Detection of Ring Structure

ÖZ

DAĞITIM ŞEBEKESİNİN AYAĞA KALDIRILMASI VE DURUMSAL FARKINDALIK ARAÇLARININ PERFORMANSININ GELİŞTİRİLMESİ

Yılmaz, Uğur Can
Yüksek Lisans, Elektrik ve Elektronik Mühendisliği
Tez Yöneticisi: Doç. Dr. Murat Göl

Haziran 2021, 84 sayfa

Elektrik modern yaşam için hayati bir ihtiyaç olmakla birlikte yokluğunda büyük zorluklarla karşılaşılabilinmektedir. Bir dağıtım şebekesinin ayağa kaldırılabilmesi için hızlı çalışan bir karar destek mekanizması ile birlikte hata payı düşük gerçek zamanlı operasyon gerekmektedir. Dağıtım şebekesinin hızlı şekilde ayağa kaldırılması elektrik kesintisi süresini en aza indirmek için büyük önem teşkil etmektedir. Bu sebeple karar destek mekanizmasında kullanılan sistem analizinin hızlı olması da kritik öneme sahiptir. Bu tez çalışmasında, özgün ve sayısal halka yapı algılama algoritması kullanılarak şebekenin bölünmesi ile bahsedilen analizler hızlandırılmıştır. Dahası, ayağa kaldırma işlemi boyunca durumsal farkındalığı arttırmak için sistemi gerçek zamanlı olarak izleyen bir araç geliştirilmiştir. Bu araçta sahadaki enerjilendirilmiş kısımdan gelen ölçümleri işleyerek en olası sistem değişkenlerini kestiren ve ayrıca güvenilirliği düşük olan yük ve tüketim tahminlerini de güncelleyen bir durum kestirim algoritması bulunmaktadır. En Küçük Mutlak Değerler metoduyla geliştirilen durum kestirim algoritması ölçüm fonksiyonlarının lineerizasyonu ile hızlandırılmıştır. Son olarak, bahsedilen gerçek zamanlı izleme aracı verimli bir yük akış analizi kullanarak uygulanması mümkün olmayan ayağa kaldırma stratejilerini belirlemektedir.

Anahtar Kelimeler: Dağıtım Şebekesi Ayağa Kaldırma, Üç Faz Durum Kestirimi, Durumsal Farkındalık Araçları, İleri Geri Yük Akışı Analizi, Halka Yapı Algılama

To my beloved family

Süreyya Yılmaz

Memet Hanifi Yılmaz

İmge, Kerime, Onur Can Yılmaz

ACKNOWLEDGMENTS

I would like to express my deepest gratitude to my supervisor Assoc. Prof. Murat Göl for his guidance, advice, criticism, encouragement, and insight throughout the research. Prof. Gol has been a mentor to me for 4 years, and I am grateful for his support and wisdom.

I also would like to thank Asst. Prof. Ebru Gol, Asst. Prof. Burcu Güldür, Onur Yiğit Arpali and Merve Bayraktar who are the other researchers of the TUBITAK project. It has been my pleasure to work with these ambitious researchers.

All the friends in the E101 research laboratory have taught and supported me. I would like to thank Mustafa Erdem Sezgin on behalf of all the researchers in the laboratory.

This work is funded by Scientific and Technological Research Council of Turkey under grant number TUBİTAK 118E183 and BIDEB 2210-A funding.

I would like to thank Arda Otlu for being my brother for 15 years,

I would like to thank Deniz Yazıcıoğlu for being for a sincere friend to me.

I would like to thank Narmin İbrahimli for being my part time lover.

Lastly, I would like to thank my family for their incredible support. They have always been more supportive and loving to me than I could ever imagine. I would like to dedicate my degree to all their sacrifice.

TABLE OF CONTENTS

LIST OF TABLES

TABLES

LIST OF FIGURES

FIGURES

LIST OF ABBREVIATIONS

SCADA	Supervisory Control And Data Acquisition
MDP	Markov Decision Process
DRS	Detection of Ring Structure
IRS	Identification of Ring Structure
PMU	Phasor Measurement Unit
NR	Newton- Raphson
GS	Gauss-Seidel
FDLF	Fast Decoupled Load Flow
FBPF	Forward-backward power flow
LAV	Least Absolute Values
WLS	Weighted Least Squares
LP	Linear Programming
MCB	Minimum Cycle Basis
BIBC	Bus Injection to Bus Current
Y_{bus}	Bus Admittance Matrix
RDE	Ring system Detection and Extraction
MSE	Mean Squared Error
MAPE	Mean Absolute Percentage Error

CHAPTER 1

INTRODUCTION

Electricity has a crucial role in modern life, and its absence may cause catastrophic complications. The main objective of the power distribution system operators is to provide uninterrupted and stable electricity to its customers. Although power distribution networks are designed and maintained to prevent interruption in the electricity service, partial or full blackouts are unavoidable considering extraordinary situations, e.g., disasters, faults, etc. When the electricity supply is interrupted by an unexpected cause, it is imperative to restore the power distribution network in a fast manner. A restoration problem can be formulated as a multi-objective, multi-stage, combinatorial, nonlinear, and constrained optimization problem [1].

Although there are comprehensive studies in the transmission system restoration, restoration of the distribution systems has some research gaps. To better understand the difference in the transmission and distribution system restorations, the divergence in the characteristic of those systems should be investigated. Distribution systems differ from transmission networks due to the lack of measurements, the number of buses, unbalanced loads and structure, lack of transposition, and high R/X ratio. The size of the system in the distribution networks may be thousands of buses which makes the system analysis computationally expensive. In addition to that, the situational awareness for the distribution system requires a tool that is capable of processing three-phase measurements considering the unbalanced variables, being robust against bad (biased) data considering the lack of measurements, preventing the ill-conditioning considering high R/X ratio in the flow analysis. To address the given complications, this thesis proposes an efficient partitioning method and an

improved situational awareness tool to be utilized in the distribution system restoration. The overall restoration procedure is shown in the flow chart given in Figure 1.1. The contribution of this work is presented in two modules which are shown in green in the flow chart. The first module, partitioning of distribution system topology, is developed to improve the computational performance of the restoration process. The second module, the situational awareness tool, is developed to monitor the system in real-time using field measurements and to conduct a feasibility analysis for the given restoration strategies using the available generation and load forecasts/profiles.

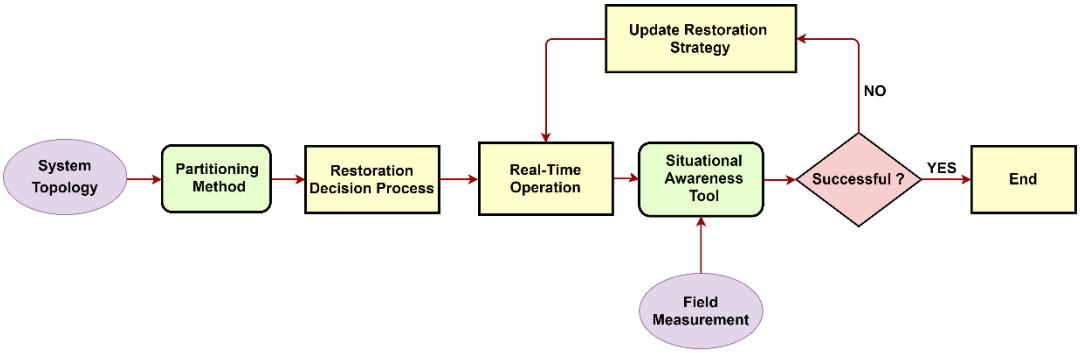

Figure 1.1. The flow chart of the restoration procedure.

Although the synthesis of the restoration strategy is out of the scope of this thesis, the factor causing the computational complexity should be highlighted to understand the proposed method better. The restoration strategy of a fully radial structure is straightforward such that buses are tried to be energized in a sequential order starting from the source side. However, when ring structures are considered, there are more than one restoration path to energize the buses. Thus, by partitioning the system into ring and radial structured buses, the restoration strategy can be developed separately. Therefore, a novel partitioning algorithm is proposed in this thesis to improve the performance of the restoration process.

The situational awareness tool for the distribution system during the restoration is the second module of the proposed methodology. The distribution system is not fully observable due to the lack of measurements, hence unreliable forecasts and profiles have to be utilized to maintain system observability. The reliable real-time three-phase measurements gathered from the energized part of the field and unreliable forecasts/profiles of the un-energized part should be both processed to execute power analysis methods so that the electrical constraints can be included in the restoration optimization problem.

In this thesis, the research gaps related to the inclusion of the electrical constraints and the computational performance are addressed. A novel numeric analysis to detect ring and radial structures is proposed to improve the computational time of the restoration by partitioning the system. Furthermore, a situational awareness tool is developed to improve the situational awareness. This tool utilizes a state estimator to process the real-time measurements gathered from the energized section of the field and to estimate the most likely system states, i.e., bus voltage magnitudes and phase angles. An efficient power flow method is also employed to analyze the whole system using load and generation forecasts/profiles.

1.1 Problem Definition

While the restoration methodology of the transmission networks has been comprehensively studied by various researchers [2]–[4], there are still some research gaps to be addressed in the distribution system restoration considering the lack of proper monitoring, the number of buses with domain-specific topology, and the tendency of unbalanced operation of distribution networks [5]–[7].

In this thesis, a generic performance improvement of the restoration and situational awareness for the distribution system is the main focus; in addition, situational awareness for the distribution system exposed to a disaster is also considered. After a disaster, the unbalanced operation may be significantly noticeable compared to the

normal operation. The restoration of a distribution system is studied by various researchers [8]–[10]. Even the restoration of undamaged networks requires systematic policy, restoration of the power networks exposed to a disaster may be challenging. Ref. [8] propose a restoration method to guide the field crew however, electrical constraints are not included in the problem formulation. In [9], a probabilistic approach to the restoration procedure is proposed. [10] enriches [9] by including electrical constraints using power flow. The given methods are offline methods such that the restoration action set is determined once, and it is not updated with the real-time measurements gathered from the energized sections.

The restoration strategy of a fully radial structure is straightforward such that buses are tried to be energized in a sequential order starting from the source side. However, when ring structures are considered, there are more than one restoration path to energize all buses. The combinatorial nature of the problem is caused by the numerous 0-1 variables corresponding to the switching devices. In addition, the majority of a distribution network infrastructure is radial structured. If the restoration strategy for the radial structured and ring structured parts of the system are developed separately, the computational performance would be improved significantly. Therefore, an efficient method to detect ring and radial structured sections should be utilized in the restoration process.

Consider three different configurations of the distribution system topology given in Figure 1.2. While the topology given in Figure 1.2a shows a radial structure with connection to the transmission network, Figure 1.2b and Figure 1.2c shows ring structured configurations. In Figure 1.2b, intuitively ring structured branches can be observed while in Figure 1.2c the corresponding branches constitute a ring structure since transmission network connection is assumed to be an infinite source. In the partition algorithm, it is important to detect both ring structures given in Figure 1.2b and Figure 1.2c.

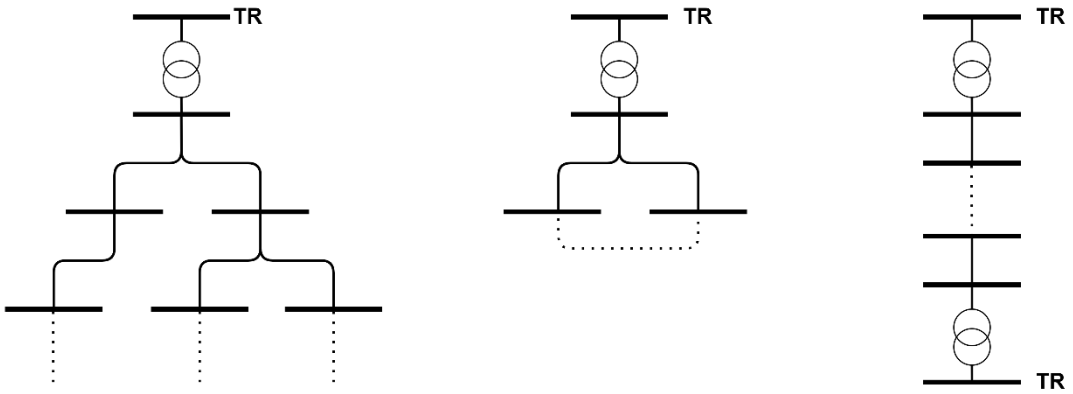

(a) (b) (c)

Figure 1.2. Various configuration of the distribution system topology

Conventionally, graph theoretic methods have been widely utilized to identify the topology of a power system [11]. However, as the size of the power systems increases, those studies lose the feasibility to analyze the system in a reasonable time. With the developments in renewable sources and electrical vehicles, real-time monitoring and control of the distribution system became essential in recent years. Thereby, there are various studies on topology analysis of distribution systems [12]–[14]. Considering the size of the distribution network can be up to thousands of buses, the given graph based methods are not capable of analyzing the system in a reasonable time. While [15] proposes reduced computational complexity of the topology identification, they have been employed in small-sized systems, and the performance of the proposed method on a real-sized distribution system is not given.

Once the restoration strategy is obtained, the real-time operation takes place to energize the buses. During the real-time operation, real-time monitoring of the system is critical to observe the system states, i.e., bus voltage magnitudes and phase angles. The bus voltage magnitude limitations and power flow limitations should be satisfied in the distribution system. Bus voltage magnitudes should be in the limits

of 0.95-1.05 pu, and power flows should be lower than the maximum power flow capacity of the corresponding line.

In the energized sections of the system, three-phase reliable measurements are obtained by SCADA devices. On the other hand, distribution systems suffer from the lack of measurements. To maintain full system observability, pseudo injection measurements are inserted using load and generation forecasts/profiles. Unlike real-time measurements, forecasts and profiles are unreliable, and they can be even more biased in the distribution systems exposed to an unexpected situation. Considering the available measurements, the situational awareness tool using both power flow analysis and state estimation method is required to properly monitor the distribution system during restoration.

State estimation tool is essential to process the real-time measurements gathered from the energized section of the field. Since the pseudo measurements are also utilized, the estimator is supposed to be robust against bad data. Furthermore, the computational time of the estimation should be considered. As the branches energized step by step, the state estimation algorithm can be executed for the energized parts of the system to find system states, i.e., bus voltage magnitudes and bus voltage phase angles.

In the transmission networks, the positive sequence model of the system can be employed in the state estimation algorithm thanks to balanced load and structure profiles. Besides the fact that the normal operation of the distribution system may suffer from lack of transposition, unbalanced loads, and high R/X ratio [16], [17], unbalanced operation tends to be more obvious in a collapsed distribution network. Thereby, the three-phase state system model is essential to obtain accurate results [18]–[20].

Lastly, using the state estimation method, the violation of electrical constraints in the energized part of the system can be detected. However, it is also important to predict and foresee the possible violations that can occur if the restoration strategy is realized in the field. This approach prevents the application of an infeasible action set. During

the restoration, power flow analysis can be conducted for the whole system using pseudo injection measurements. Considering the size of the distribution systems, the power flow analysis should be efficient. As some of the buses are energized, pseudo injection measurements can be replaced with the injection measurement values estimated by the state estimation tool. Thus, it can be said that the reliability of the power flow analysis improves as the size of the energized section increases. To sum up, the power flow analysis and state estimation tool can be utilized together to detect both operational violations and predicted possible violations in the distribution system during restoration.

1.2 Scope and Contribution of the Thesis

In this thesis, topology, power flow, and state estimation analyses of the distribution network are studied to be employed in an online decision support mechanism to restore the network. While topology analysis aims to improve the computational time performance of the restoration, power flow and state estimation tools are developed to inspect the electrical constraints during the restoration and modify the restoration strategy if required.

The restoration of the distribution network is studied in a multidisciplinary project funded by Scientific and Technological Research Council of Turkey under grant number TUBİTAK 118E183 where the scope of this thesis is to develop an efficient numeric algorithm to detect the ring structure to improve the computational performance of the restoration and to implement power flow, state estimation algorithms to consider electrical constraints throughout the restoration process. The restoration strategy is obtained using Markov Decision Process (MDP). The Detection of Ring Structure (DRS) method is employed in the partitioning method whereas power flow and state estimation algorithms are utilized in the situational awareness tool. Once the action sequence is obtained by MDP, the branches are energized step by step according to the proposed action sequence. The feasibility of each action set is validated using the power flow results, and state estimation is

utilized in the energized part to find system states, i.e., bus voltage magnitudes and phase angles using real-time measurements. The pseudo injection measurements of the energized part are updated using the results of state estimation. It is aimed to detect any possible violation of electrical constraints by running power flow at each step. On the other hand, state estimation results yield any violation of electrical constraints in the energized part. In the following sub-sections, the detailed literature survey and the scope of the proposed methods are presented.

1.2.1 Detection of Ring Structure

To improve the computational performance of the restoration process, the ring and radial structured buses are required to be detected. In this thesis, a novel numeric DRS method is presented. The proposed method aims to detect ring and radial structured buses in an efficient manner. Note that while the DRS stands for the classification of the buses into two main groups, namely ring structured and radial structured buses; Identification of Ring Structure (IRS) yields each independent ring structure and its elements. The performance of the proposed DRS method is further improved with a pre-process named strategical ordering. Furthermore, besides the restoration application, the proposed DRS method can also be employed in the IRS. Instead of utilizing graph based methods for the whole distribution system, only ring structured buses can be analyzed with graph theoretic methods to reduce the computational time significantly.

The effect of the proposed DRS method in the restoration of sample systems is given in Chapter 5 as well as the computational performance results of the IRS method with/without DRS.

1.2.2 Distribution System Power Flow

The outcome of the restoration strategy is a set of actions that reveals the sequence and path of the buses to be energized. Once the restoration actions are obtained, they

require a feasibility check before the real-time operation takes place. Therefore, an efficient power flow analysis should be employed in the situational awareness tool during the restoration. The power flow analysis uses load and generation profiles/forecasts. Considering the load and generation profiles/forecasts are obtained for the single-phase equivalent model, power flow analysis is also developed for the single-phase equivalent model of the distribution network.

There are various power flow analysis methods in the literature, namely Newton-Raphson (NR), Gauss-Seidel (GS), fast decoupled load flow (FDLF) [16], [21]. GS method is the most uncomplicated and authentic method whereas construction of Jacobian matrix at each iteration in the NR method causes computational burden. The convergence of the GS method is completely linear; however, the system size and the computational time are proportional to each other that is the increasing system size causes a poor convergence rate whereas the NR method has a convergence of quadratic type [22]. The distribution system falls in the category of ill-conditioned power systems due to the following features for the given flow analysis methods, and both NR and GS methods have convergence issues due to the ill-conditioned system [23].

- Radial or weakly meshed networks
- High R/X ratio
- Unbalanced operation

On the other hand, the forward-backward power flow (FBPF) is developed by W.H.Kersting [24] and R.Berg [25] to be utilized in the radial distribution systems. The approach, known as the modified Ladder iterative technique, involves forward and backward sweeps through the network using Kirchoff's voltage and current laws. Moreover, J.H Teng [26] proposed the direct method (BIBC/BCBV matrix method) to improve the computational performance of FBPF where the methodology is the same; however, the data storage method is modified. Bus Injection to Branch Current (BIBC) and Branch Current to Bus Voltage (BCBV) matrices are utilized in the method where the flow analysis can be conducted without using the NR methods.

Among those methods, FBPF using BIBC/BCBV matrix method is employed in the situational awareness tool considering the radial structure and high R/X ratio of the distribution networks [27].

Furthermore, under the assumption that DERs do not control the voltage, in other words, they operate with a constant power factor, DERs can be modeled as negative power demand loads. On the other hand, if a DER is the only source of an island operating part, it is expected to control the voltage.

1.2.3 Distribution System State Estimation

Once the restoration strategy is determined, the real-time operation takes place. The buses are energized according to the restoration action set. The energized section of the system requires a situational awareness tool that is capable of analyzing unbalanced measurements. Thereby, in this thesis, a three-phase Least Absolute Values (LAV) based state estimator is developed.

The transmission network is known to have a balanced structure and loading whereas it is not guaranteed in the distribution system due to unbalanced loads, lack of transposition, and unbalanced structure [28]. Moreover, the proposed situational awareness tool is expected to be employed in the restoration of a distribution system exposed to a disaster. Therefore, the proposed estimator is required to be implemented using the three-phase model of the system to monitor the system accurately [29].

Weighted Least Squares (WLS) is the most common method to be utilized in the transmission state estimation. However, it is vulnerable to bad data and it requires additional bad data detection and identification otherwise, the bad data can bias the estimator result significantly [30]. Considering the lack of observability of the distribution networks, pseudo injection measurements are commonly utilized to maintain full system observability. Thus, a robust estimator against bad data is essential to obtain accurate results considering there are unreliable pseudo injection

measurements in the system. LAV based state estimator automatically rejects bad data since it uses the minimum number of measurements which minimizes the error.

1.2.4 Contribution of the Thesis

The contributions of this thesis are listed as follows.

- An efficient and novel numeric DRS method to improve the computational performance of the restoration process is proposed. Moreover, a pre-process, namely strategical ordering, is proposed to further improve the computational performance of the detection algorithm.
- An efficient FBPF algorithm is implemented to obtain any possible violation of the given restoration path.
- LAV based three-phase state estimation algorithm is implemented to obtain system states of the distribution network. Using the obtained system states, any violation of electrical constraints can be detected in the restored distribution network.
- The performance of the state estimation is improved by partial linearization of the measurement functions.

1.3 Thesis Outline

In this thesis, the work is presented in six chapters. The structure of the thesis is given as follows.

The first chapter is the introduction where the problem is defined, and the scope of this thesis is explained. Moreover, the literature review of the related works is provided, and the contributions of this study are itemized. To sum up, the research gap in the literature and how to address the gap are revealed in this chapter.

The second chapter yields background information. Since this study employs a state estimator, the methodology of LAV based single-phase state estimation method is

summarized in this chapter. Similarly, the theoretic background of the Cholesky factorization is given in the second chapter since its modified version is employed in the proposed DRS method.

The proposed DRS algorithm and situational awareness tool are given in Chapters 3 and 4, respectively. In Chapter 3, the methodology of the proposed DRS method is explained, and additional usage of the method in the IRS is given. In Chapter 4, the developed power flow analysis and state estimation method to be utilized in situational awareness are explained. The methodology of the forward/backward power flow analysis and LAV based three-phase state estimation are given in this chapter. The details of the estimation method selection are also summarized in one sub-section.

Chapter 5 includes the validation of the proposed methods. In the chapter, various test cases are included to compare the numeric results.

In the conclusion which is the last chapter, the aim and success of this work are summarized. Also, future work to improve situational awareness further in the distribution network restoration is indicated.

CHAPTER 2

BACKGROUND INFORMATION

In Introduction Chapter, the restoration of the power system concept is presented. The main challenges of a restoration process are highlighted, then, the proposed methods to address those challenges are provided. While defining the problem, the literature survey is conducted to reveal the current status of power system restoration studies. Moreover, the literature review on detection of ring structures, distribution system power flow analysis, and state estimation are also included. The first chapter is concluded with the contribution of this thesis.

This chapter introduces the technical background of the proposed algorithms to provide the audience a better understanding. The situational awareness tool requires a robust and efficient state estimator. The basic concept of state estimation in a power system is given in this chapter. In the following chapters, the estimator is computationally improved, and the three-phase model is utilized. The mathematical background of the estimation measurement function and LAV based optimization problem are explained in Chapter 2.1. Furthermore, in the proposed DRS method, a modified Cholesky factorization, namely incomplete Cholesky factorization is utilized. Thus, the basic concept of the Cholesky factorization is presented in Chapter 2.2 so that the usage of incomplete Cholesky factorization in the DRS method can be followed easily.

2.1 Least Absolute Values Estimation

State estimation in the power system is firstly proposed by Fred Schweppe [31]–[33]. The utilization of state estimation improved the capabilities of the SCADA, subsequently, Energy Management System (EMS) concept is revealed thanks to

online state estimation. Although recent studies cover dynamic estimators, the scope of this thesis is limited to static estimators which operate for a given time instant.

There are various state estimation methods in the literature depending on the optimization objective. In this study, LAV based states estimation method is preferred, the details of the selection of this method will be investigated in the following chapters.

LAV estimator obtains the system states namely, the magnitude of bus voltage and phase angle of bus voltages by utilizing real-time measurements. The measurements can be collected by either SCADA or PMU. PMU measurements are not taken into account in this study since the portion of PMU measurements is significantly low compared to SCADA measurements. SCADA measurements can be active and reactive power injection measurements, power flow measurements, and voltage magnitude measurements.

The basic operation of the transmission system state estimation is designed under certain assumptions [30]. The power system is assumed to be balanced, and it operates in steady state. Using the assumption, all system components and system states are modeled using the positive sequence model of the system. Furthermore, measurement errors are assumed to be independent, i.e., $E\{e_i e_j\} = 0$.

The measurement model for the estimator is given in equation 2.1.

$$z = \begin{bmatrix} z_1 \\ z_2 \\ \vdots \\ z_m \end{bmatrix} = \begin{bmatrix} h_1(x_1, x_2, \dots, x_n) \\ h_2(x_1, x_2, \dots, x_n) \\ \vdots \\ h_m(x_1, x_2, \dots, x_n) \end{bmatrix} + \begin{bmatrix} e_1 \\ e_2 \\ \vdots \\ e_m \end{bmatrix} = h(x) + e \qquad (2.1)$$

where, $h_i(x)$ is the non-linear function relating measurement i to the state vector x, z is the set of measurements, e is the vector of measurement errors, and x is the vector of system states. The size of z vector is $(mx1)$ where m is the number of measurements and the size of x vector is $(nx1)$ where n is the number of states.

The objective function of the LAV based estimation is given in equation 2.2.

$$\begin{aligned} &\text{minimize} \quad \sum_{i=1}^{m} |r_i| \\ &\text{subject to} \quad z_i = h_i(x) + r_i\,, \qquad 1 \le i \le m \end{aligned} \tag{2.2}$$

where, r_i is the residual of i^{th} measurement corresponding to the difference between the real value of the measurement and the estimated value of the measurement, i.e., $r_i = z_i - h(\hat{x}_i)$. If x^0 is assumed to be the initial solution, first-order approximation of $h_i(x^0)$ around x^0 can be solved using a set of linear programming (LP) problems. Thus, the objective function is reorganized for the LP solution as shown in equation 2.3.

$$\begin{aligned} &\text{minimize} \sum_{i=1}^{m} \left(u_i^k + v_i^k\right) \\ &\text{subject to } H \cdot \Delta x_u - H \cdot \Delta x_v + u - v = \Delta z \\ &\Delta x_u, \Delta x_v, u, v \ \ge 0 \end{aligned} \tag{2.3}$$

where,

$\Delta x = \Delta x_u - \Delta x_v$

$u_i^k - v_i^k = z - h(x^k) - H(x^k) \cdot \Delta x = \Delta z^k - H(x^k) \cdot \Delta x^k$, and it is equal to the measurement residual at the k^{th} iteration.

Furthermore, the problem can be written as a standard LP problem as shown in equation 2.4.

$$\begin{aligned} &\text{minimize} \quad c^T \cdot Y \\ &\text{subject to} \quad A \cdot Y = b \\ &\qquad\qquad Y \geq 0 \end{aligned} \tag{2.4}$$

where,

$c^T = [0_n, 0_n, 1_m, 1_m]$,

0_n : a zero vector of order n,

1_m : a vector of order m, where all the entries are 1,

$b = \Delta z$,

$Y^T = [\Delta x_u^T, \Delta x_v^T, u^T, v^T]$,

$A = [H, -H, I_m, -I_m]$,

I_m : an identity matrix of order m.

To solve equation 2.4, a simplex based optimization algorithm is utilized. When $|\Delta x|$ becomes less than a predefined threshold value, the algorithm is said to be converged. To derive the measurement Jacobian matrix, H, firstly the measurement function, $h(x^k)$, should be obtained for each measurement type. The relation of the measurements with respect to the states is given in equations 2.5–2.8.

$$P_i = V_i \cdot \sum_{j \epsilon N_i} V_j \cdot (G_{ij} \cos(\theta_{ij}) + B_{ij} \sin(\theta_{ij})) \tag{2.5}$$

$$Q_i = V_i \cdot \sum_{j \epsilon N_i} V_j \cdot \left(G_{ij} \sin(\theta_{ij}) - B_{ij} \cos(\theta_{ij})\right) Y \geq 0 \tag{2.6}$$

$$P_{ij} = {V_i}^2 \cdot \left(g_{si} + g_{ij}\right) - V_i \cdot V_j \cdot \left(g_{ij} \cdot \cos(\theta_{ij}\right) + b_{ij} \cdot \sin(\theta_{ij})) \tag{2.7}$$

$$Q_{ij} = -{V_i}^2 \cdot \left(b_{si} + b_{ij}\right) - V_i \cdot V_j \cdot \left(g_{ij} * \sin(\theta_{ij}\right) - b_{ij} \cdot \cos(\theta_{ij})) \tag{2.8}$$

where,

V_i , θ_i : the voltage magnitude and phase angle at bus i ,

θ_{ij} : $\theta_i - \theta_j$,

$G_{ij} + jB_{ij}$: ij^{th} element of the complex bus admittance matrix,

$g_{ij} + jb_{ij}$: the admittance of the series branch connecting buses *i* and *j*,

$g_{si} + jb_{si}$: the admittance of the shunt branch connected to bus *i*,

N_i : the set of buses that are directly connected to bus *i*.

The measurement Jacobian matrix, H, is formed using the derivatives of the measurement functions with respect to the system states. The structure of H matrix is given in equation 2.9.

$$H = \begin{bmatrix} \frac{\partial P_{inj}}{\partial \theta} & \frac{\partial P_{inj}}{\partial V} \\ \frac{\partial P_{flow}}{\partial \theta} & \frac{\partial P_{flow}}{\partial V} \\ \frac{\partial Q_{inj}}{\partial \theta} & \frac{\partial Q_{inj}}{\partial V} \\ \frac{\partial Q_{flow}}{\partial \theta} & \frac{\partial Q_{flow}}{\partial V} \\ 0 & \frac{\partial V_{mag}}{\partial V} \end{bmatrix} \tag{2.9}$$

The rows of the H matrix represent measurements whereas the columns represent the system states. The formulations of the derivates are given as following.

- Elements corresponding to real power injection measurements:

$$\frac{\partial P_i}{\partial \theta_i} = \sum_{j=1}^{N} V_i V_j\left(-G_{ij}sin\theta_{ij} + B_{ij}cos\theta_{ij}\right) - V_i^2 B_{ii}$$

$$\frac{\partial P_i}{\partial \theta_j} = V_i V_j\left(G_{ij}sin\theta_{ij} - B_{ij}cos\theta_{ij}\right) \tag{2.10}$$

$$\frac{\partial P_i}{\partial V_i} = \sum_{j=1}^{N} V_j(G_{ij}cos\theta_{ij} + B_{ij}sin\theta_{ij}) + V_i G_{ii}$$

$$\frac{\partial P_i}{\partial V_j} = V_i\left(G_{ij}cos\theta_{ij} + B_{ij}sin\theta_{ij}\right)$$

- Elements corresponding to reactive power injection measurements:

$$\frac{\partial Q_i}{\partial \theta_i} = \sum_{j=1}^{N} V_i V_j\left(G_{ij}cos\theta_{ij} + B_{ij}sin\theta_{ij}\right) - V_i^2 G_{ii}$$

$$\frac{\partial Q_i}{\partial \theta_j} = V_i V_j\left(-G_{ij}cos\theta_{ij} - B_{ij}sin\theta_{ij}\right) \tag{2.11}$$

$$\frac{\partial Q_i}{\partial V_i} = \sum_{j=1}^{N} V_i V_j\left(G_{ij}cos\theta_{ij} + B_{ij}cos\theta_{ij}\right) - V_i B_{ii}$$

$$\frac{\partial Q_i}{\partial V_j} = V_i V_j\left(-G_{ij}cos\theta_{ij} - B_{ij}sin\theta_{ij}\right)$$

- Elements corresponding to real power flow measurements:

$$\frac{\partial P_{ij}}{\partial \theta_i} = V_i V_j\left(g_{ij}sin\theta_{ij} - b_{ij}cos\theta_{ij}\right)$$

$$\frac{\partial P_{ij}}{\partial \theta_j} = -V_i V_j\left(g_{ij}sin\theta_{ij} - b_{ij}cos\theta_{ij}\right) \tag{2.12}$$

$$\frac{\partial P_{ij}}{\partial V_i} = -V_j\left(g_{ij}cos\theta_{ij} + b_{ij}sin\theta_{ij}\right) + 2\left(g_{ij} + g_{si}\right)V_i$$

$$\frac{\partial P_{ij}}{\partial V_j} = -V_i\left(g_{ij}cos\theta_{ij} + b_{ij}sin\theta_{ij}\right)$$

- Elements corresponding to reactive power flow measurements:

$$\begin{aligned}\frac{\partial Q_{ij}}{\partial \theta_i} &= -V_i V_j\left(g_{ij}cos\theta_{ij} + b_{ij}sin\theta_{ij}\right)\\ \frac{\partial Q_{ij}}{\partial \theta_j} &= V_i V_j\left(g_{ij}cos\theta_{ij} + b_{ij}sin\theta_{ij}\right)\\ \frac{\partial Q_{ij}}{\partial V_i} &= -V_i\left(g_{ij}sin\theta_{ij} - b_{ij}cos\theta_{ij}\right) - 2V_i\left(b_{ij} + b_{si}\right)\\ \frac{\partial Q_{ij}}{\partial V_j} &= -V_i\left(g_{ij}sin\theta_{ij} - b_{ij}cos\theta_{ij}\right)\end{aligned} \tag{2.13}$$

- Elements corresponding to voltage magnitude measurements:

$$\frac{\partial V_i}{\partial V_i} = 1, \frac{\partial V_i}{\partial V_j} = 0, \frac{\partial V_i}{\partial \theta_i} = 0, \frac{\partial V_i}{\partial \theta_j} = 0 \tag{2.14}$$

2.2 Cholesky Factorization

The Cholesky factorization is a particular form of factorization. It is utilized to decompose a symmetrical and positive definite matrix into the product of a lower triangular matrix and its conjugate transpose [34]. If A is positive definite $n\ x\ n$ matrix, it can be decomposed as shown in equation 2.15.

$$A = \begin{bmatrix} d_1 & a_1^T \\ a_1 & B_1' \end{bmatrix} = \begin{bmatrix} \sqrt{d_1} & 0 \\ \frac{a_1}{\sqrt{d_1}} & I_{n-1} \end{bmatrix} \cdot \begin{bmatrix} 1 & 0 \\ 0 & B_1' - \frac{a_1 * a_1^T}{d_1} \end{bmatrix} \cdot \begin{bmatrix} \sqrt{d_1} & \frac{a_1^T}{\sqrt{d_1}} \\ 0 & I_{n-1} \end{bmatrix} \tag{2.15}$$

where;

$A = L_1 \cdot A_1 \cdot L_1^T$

$A_1 = \begin{bmatrix} 1 & 0 \\ 0 & B_1 \end{bmatrix}$

Following the same procedure, A_1 can be also decomposed into $A_1 = L_2 * A_2 * L_2^T$ and at the n^{th} step, A_n will be equal to $L_n * I * L_n^T$. Thus, A matrix can be decomposed into a lower triangular matrix and its transpose as shown in equation 2.16.

$$A = L_1 \cdot L_2 \ \dots \ L_n \cdot I \cdot L_n^T \ \dots \ L_2^T \cdot \ L_1^T = L \cdot L^T \tag{2.16}$$

The basic algorithm to obtain the upper triangular matrix is given in Algorithm 1 where *n* is the column number of *A* matrix.

Algorithm 1 Cholesky Decomposition

1: ***for*** $j = 1{:}\,n$
2: ***for*** $i = 1{:}\,(j-1)$
3: $R_{ij} = (A_{ij} - \sum_{k=1}^{i-1} R_{ki} \cdot R_{kj}\ ) \,/ R_{ii}$
4: ***end***
5: $R_{jj} = \left(A_{jj} - \sum_{k=1}^{j-1} R_{kj}^2\right)^{½}$
6: ***end***

The resultant matrix, *R* , is the upper triangular matrix. Thus, the original matrix *A* can be obtained using equation 2.17.

$$A = R^T \cdot R \tag{2.17}$$

CHAPTER 3

PARTITIONING OF THE DISTRIBUTION SYSTEM TOPOLOGY

In Chapter 2, the theoretical background of the proposed methods is provided. Apart from the concept of state estimation in power systems, the algorithm of Cholesky factorization is presented in the chapter. In the third chapter of this thesis, a novel method to partition the distribution system is given where the partitioning is accomplished by detecting the ring and radial structures using incomplete Cholesky decomposition.

Restoration of a distribution system requires an efficient decision support mechanism and an accurate real-time operation. The proposed efficient partition method improves the computational performance of the decision making procedure of restoration.

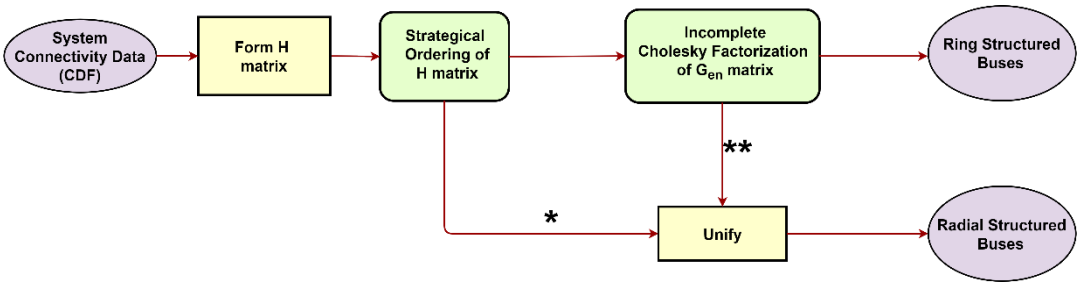

Figure 3.1. Flow diagram of the DRS method.

The proposed method detects the radial structures in two steps. While strategical ordering detects the radial structures incident to a leaf node, the result of the factorization yields the remaining radial structures. In the flow chart given in Figure 3.1, (*) corresponds to the radial structure incident to a leaf node while (**) represents the radial structures whose both ends are incident to either a ring structure

or transmission network. A leaf node can be defined as a bus connected with only one branch. The details of those 2 types of radial structures are given in Chapter 3.1.1.

While the restoration strategy for a fully radial structure is straightforward such that the buses are energized in a sequential order starting from the source side, the possible restoration actions increase exponentially in the meshed structure due to the combinatorial possibilities of the restoration path. In other words, while there is only one restoration path for a fully radial structure, each ring structure contributes a combinatorial possibility. Therefore, the radial structured part which is the majority of the system can be processed separately in restoration decision making by partitioning the system into ring and radial structured parts using the proposed numeric DRS algorithm. To do so, as shown in Figure 3.1, firstly a Jacobian matrix is formed where measurements are power injections of the buses and states are the line flows. Then, a pre-process, namely strategical ordering is employed to detect the leaf branches with no connection to the transmission network. The remaining radial structures are obtained by analyzing linear dependency of the Jacobian matrix where computationally fast incomplete Cholesky method is employed to conduct the analysis. Finally, ring structured branches are detected by decomposing the Jacobian matrix, and radial structured branches are detected by unifying the results of factorization and strategical ordering. The details of the proposed method are explained in the following sub-sections in detail.

3.1 Detection of Ring Structure

To detect the ring structures in a power network, there are numerous methods where graph based methods are employed recurrently [35]–[37]. As the size of the distribution systems increases, the utilization of those methods becomes infeasible to analyze the system in a reasonable time. Thus, a novel numerical method is proposed in this study to address the computational challenge. The proposed method includes a pre-process, namely strategical ordering, to further improve the

computational performance. Note that the aim of this numeric method is neither to obtain the number of the rings nor the bus list of each ring structure. The aim is to divide the buses into two categories, radial structured buses and ring structured buses.

The numeric method is developed based on the state estimation concept. Consider a distribution system with no interruption, such that all customers receive power. Assume that all the lines are energized, i.e., there are no open lines, and all tie-lines are closed. Provided that each bus has an injection measurement, the relation between injection measurements and line flows can be formulated as shown in equation 3.1.

$$\mathrm{z} = \mathrm{H} \cdot \mathrm{x} + \mathrm{e} \tag{3.1}$$

$$\hat{x} = (H^T \cdot H)^{-1} \cdot H^T \cdot z \tag{3.2}$$

where,

z : measurement vector $(n \times 1)$,

x : system true state vector $(b \times 1)$, where the states are the line flows,

e : measurement error vector $(n \times 1)$,

$\hat{x}$: estimated system states vector $(b \times 1)$,

H : Jacobian matrix $(n \times b)$,

n : number of buses,

b : number of branches.

Unique calculation of the line flow in equation 3.2 implies that the status of that line can be known uniquely. Using this information, the gain matrix, $G_{sys} = (H^T \cdot H)$ is investigated to reveal the uniquely identifiable branch status.

If there is a virtual power injection measurement at each bus and there is no line flow measurement as mentioned, the branches corresponding to the linearly dependent rows of the G_{sys} matrix constitute a ring structure. In a fully radial system, it is expected to identify all the branch status uniquely since all rows of the G_{sys} matrix are linearly independent.

To obtain linearly dependent rows of G_{sys} matrix, row reduced echelon form of the matrix can be calculated. However, considering the size of the gain matrix due to the great number of buses in the distribution system, this process can be inefficient to be utilized in the real-time application. Instead of the row reduced echelon form, detection of linearly dependent/independent rows of G_{sys} matrix is accomplished by a novel numeric method to reduce the computational time significantly. Moreover, strategical ordering is utilized to pre-process the G_{sys} matrix to improve the performance further.

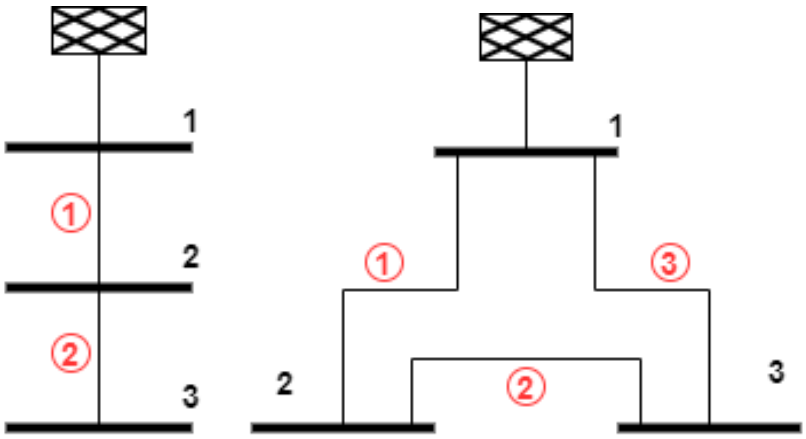

(a) (b)

Figure 3.2. Sample Systems in (a) Radial and (b) Ring Structured Topology.

To better illustrate the relation between linearly dependent rows of G_{sys} matrix and branches that are constituting a ring structure, two sample systems are given in

Figure 3.2. In Figure 3.2a, a three bus fully radial system is shown where the injection measurement at the leaf node is equal to the power flow measurement incident to the node. The corresponding Jacobian matrix, H_{rad}, is given in equation 3.3. Thus, the rows of G_{rad} matrix is expected to be linearly independent where $G_{rad} = (H_{rad}^T \cdot H_{rad})$.

The row reduced echelon form of the G_{rad} matrix yields identity matrix as expected. On the other hand, row reduced echelon form of the $G_{ring} = (H_{ring}^T \cdot H_{ring})$ proves that the rows of G_{ring} are linearly dependent where H_{ring} corresponds to the system given in Figure 3.2b.

$$H_{rad} = \begin{bmatrix} 1 & 0 \\ -1 & 1 \\ 0 & -1 \end{bmatrix}, \quad H_{ring} = \begin{bmatrix} 1 & 0 & 1 \\ -1 & 1 & 0 \\ 0 & -1 & -1 \end{bmatrix} \tag{3.3}$$

$$rref(G_{rad}) = \begin{bmatrix} 1 & 0 \\ 0 & 1 \end{bmatrix} \tag{3.4}$$

$$rref(G_{ring}) = \begin{bmatrix} 1 & 0 & 1 \\ 0 & 1 & 1 \\ 0 & 0 & 0 \end{bmatrix} \tag{3.5}$$

3.1.1 Strategical Ordering

The main aim of developing a novel DRS method is to reduce computational burden as the proposed method is utilized in a real-time application. Thus, a pre-process namely, strategical ordering, is proposed in this study to further reduce the computational time.

Using strategical ordering, the radial structures containing a leaf node are detected with a computationally cheap matrix re-ordering operation. However, after those

radial structures are detected, there are still radial structures whose both ends are incident to either a ring structure or transmission network. Thereby, incomplete Cholesky is employed to detect the remaining radial structures after strategical ordering is executed. To better illustrate the difference between those two types of radial structures, Figure 3.3 can be investigated. If the switch connected to Bus 8 is assumed to be closed, Branches 5 and 6 constitute a radial structure containing a leaf node (Bus 6), and this structure is expected to be detected using strategical ordering. On the other hand, Branches 4 and 7 constitute a radial structure whose both ends are connected to a ring structure, and this time incomplete Cholesky factorization will be employed to detect those branches.

Strategical ordering is performed while forming the corresponding Jacobian matrix of the system. The rows of H matrix represent the bus injection measurements whereas the columns represent the flow measurements. Then, the rows representing the power injection measurements of the leaf buses have only one non-zero value in the corresponding rows while all the other rows contain more than one non-zero value. If one re-order the rows and columns of the H matrix, H matrix can be partitioned into four sub-matrices as shown in equation 3.6. The buses represented by the identity matrix correspond to the leaf nodes whose rows contain only one non-zero term.

$$H = \begin{bmatrix} I & 0 \\ Y & H_{en} \end{bmatrix} \tag{3.6}$$

To further simplify the process, non-zero elements of Y sub-matrix can be replaced by zeros trivially since Y matrix is a linear combination of the identity matrix. Once Y sub-matrix is replaced with zero matrix, there may be some rows with only one non-zero value in the H_{en} sub-matrix. If H_{en} is re-ordered, some of the buses can be represented inside the identity matrix. This iterative process is repeated until there is

no row containing only one non-zero term in the H_{en} sub-matrix. This process ensures that the branches incident to the leaf nodes will not be further analyzed. Note that this pre-process is not a trace algorithm rather it is simply re-ordering of H matrix.

Consider the system given in Figure 3.3 where all the lines are closed, and all the buses are energized. Assuming there is a virtual power injection measurement at each bus, the strategical ordering can be utilized in the given sample system. The power equations for the given system are given in equations 3.7-3.11.

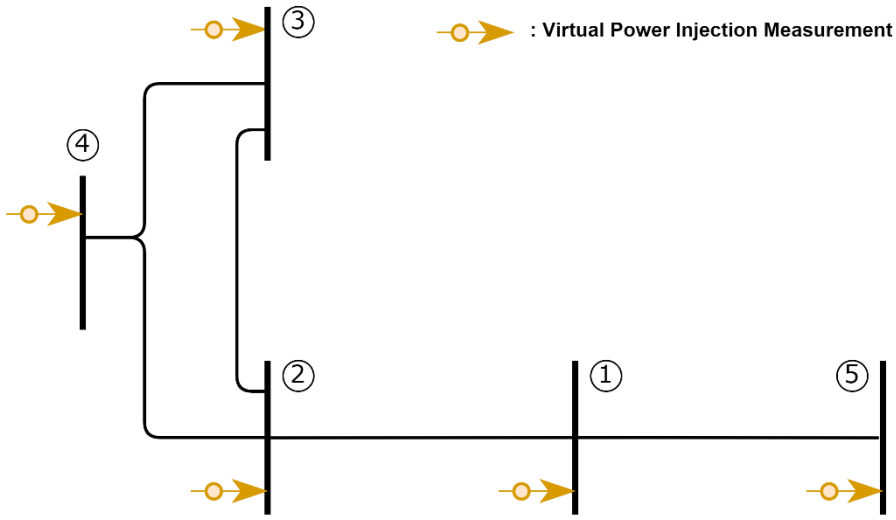

Figure 3.3. Sample 5 bus system

$$P_1 = P_{21} - P_{15} \tag{3.7}$$

$$P_2 = P_{42} + P_{32} - P_{21} \tag{3.8}$$

$$P_3 = P_{43} - P_{32} \tag{3.9}$$

$$P_4 = -P_{42} - P_{43} \tag{3.10}$$

$$P_5 = P_{15} \tag{3.11}$$

In equation 3.13, the H matrix is formed for the virtual power injection measurement at Bus-1 where the states are line flows and measurements are the virtual power injection measurements. The state vector is also given in equation 3.12.

$$x = [P_{21} \quad P_{43} \quad P_{42} \quad P_{32} \quad P_{15}] \tag{3.12}$$

$$H = \begin{array}{c} \\ P_1 \end{array} \begin{array}{c} \begin{array}{ccccc} P_{21} & P_{43} & P_{42} & P_{32} & P_{15} \end{array} \\ \begin{bmatrix} 1 & 0 & 0 & 0 & -1 \end{bmatrix} \end{array} \tag{3.13}$$

The P_2, P_3, P_4 measurements are also included in the H matrix, respectively in equations 3.14, 3.15, 3.16.

$$H = \begin{array}{c} \\ P_1 \\ P_2 \end{array} \begin{array}{c} \begin{array}{ccccc} P_{21} & P_{43} & P_{42} & P_{32} & P_{15} \end{array} \\ \begin{bmatrix} 1 & 0 & 0 & 0 & -1 \\ -1 & 0 & 1 & 1 & 0 \end{bmatrix} \end{array} \tag{3.14}$$

$$H = \begin{array}{c} \\ P_1 \\ P_2 \\ P_3 \end{array} \begin{array}{c} \begin{array}{ccccc} P_{21} & P_{43} & P_{42} & P_{32} & P_{15} \end{array} \\ \begin{bmatrix} 1 & 0 & 0 & 0 & -1 \\ -1 & 0 & 1 & 1 & 0 \\ 0 & 1 & 0 & -1 & 0 \end{bmatrix} \end{array} \tag{3.15}$$

$$H = \begin{array}{c|ccccc} & P_{21} & P_{43} & P_{42} & P_{32} & P_{15} \\ P_1 & 1 & 0 & 0 & 0 & -1 \\ P_2 & -1 & 0 & 1 & 1 & 0 \\ P_3 & 0 & 1 & 0 & -1 & 0 \\ P_4 & 0 & -1 & -1 & 0 & 0 \end{array} \tag{3.16}$$

Finally, when P_5 is included in the H matrix, the corresponding row of the P_5 measurement has only one non-zero term since the power flow of the leaf bus is equal to the power injection measurement.

$$H = \begin{array}{c|ccccc} & P_{21} & P_{43} & P_{42} & P_{32} & P_{15} \\ P_1 & 1 & 0 & 0 & 0 & -1 \\ P_2 & -1 & 0 & 1 & 1 & 0 \\ P_3 & 0 & 1 & 0 & -1 & 0 \\ P_4 & 0 & -1 & -1 & 0 & 0 \\ P_5 & 0 & 0 & 0 & 0 & 1 \end{array} \tag{3.17}$$

As the strategical ordering proposes, the matrix should be re-ordered to obtain the structure given in equation 3.6. The ordering of the state vector is modified as shown in equation 3.18, and the corresponding rows of P_1 and P_5 are replaced. Then, the re-ordered H matrix is shown in equation 3.19 where the size of the identity matrix is (1×1), and the Y sub-matrix is highlighted. Since Y matrix is a linear combination of the identity matrix, non-zero elements of Y sub-matrix can be replaced by zeros trivially.

$$x = [P_{15} \quad P_{43} \quad P_{42} \quad P_{32} \quad P_{21}] \tag{3.18}$$

$$H = \begin{array}{c|ccccc} & P_{15} & P_{43} & P_{42} & P_{32} & P_{21} \\ P_5 & 1 & 0 & 0 & 0 & 0 \\ \hline P_2 & 0 & 0 & 1 & 1 & -1 \\ P_3 & 0 & 1 & 0 & -1 & 0 \\ P_4 & 0 & -1 & -1 & 0 & 0 \\ P_1 & -1 & 0 & 0 & 0 & 1 \end{array} \quad (3.19)$$

The result of the first iteration of re-ordering yields another row with only one non-zero value considering Y sub-matrix is replaced with a zero matrix. The row corresponding to the P_1 measurement is now replaced with the row of P_2, and P_{21} line flow is replaced with P_{43}. As a result, the matrix shown in equation 3.20 is obtained where the identity matrix is (2×2). Although the Y sub-matrix is replaced with a zero matrix, there is no row containing only one non-zero term in the remaining part. The result of the strategical ordering for the 5 bus sample system yields branches between Bus 1-5 and Bus 1-2 form a radial structure containing a leaf node.

$$H = \begin{array}{c|ccccc} & P_{15} & P_{21} & P_{42} & P_{32} & P_{43} \\ P_5 & 1 & 0 & 0 & 0 & 0 \\ P_1 & 0 & 1 & 0 & 0 & 0 \\ \hline P_3 & 0 & 0 & 0 & -1 & 1 \\ P_4 & 0 & 0 & -1 & 0 & -1 \\ P_2 & 0 & -1 & 1 & 1 & 0 \end{array} \quad (3.20)$$

The branches represented by the identity matrix are said to be radial since the corresponding sub-matrix in the G_{sys} matrix is also an identity matrix that is linearly independent trivially as shown in equation 3.21. Only $G_{en} = (H_{en}^T \cdot H_{en})$ will be

investigated to obtain linearly dependent rows corresponding to the branches that are constituting ring structure.

$$G_{sys} = H^T \cdot H = \begin{bmatrix} I & 0 \\ 0 & H_{en}^T \end{bmatrix} \cdot \begin{bmatrix} I & 0 \\ 0 & H_{en} \end{bmatrix} = \begin{bmatrix} I & 0 \\ 0 & H_{en}^T \cdot H_{en} \end{bmatrix} \tag{3.21}$$

Although row reduced echelon form of G_{en} yields linear dependency of the rows, incomplete Cholesky factorization will be utilized considering computational performance. The comparison of those two methods is presented in Chapter 5.

3.1.2 Incomplete Cholesky Factorization

In Chapter 2.2, the methodology of Cholesky factorization is explained. If a matrix is singular, i.e., not full ranked, the Cholesky method fails to converge. In the proposed DRS method, it is expected to have singular G_{en} matrix if there is at least one ring structure in the system. Therefore, the incomplete Cholesky method is utilized to obtain linearly dependent/independent rows of G_{en} matrix.

As mentioned earlier, the branches represented inside the identity matrix are already marked as radial. Thus, only G_{en} will be investigated, where the relation between power injection measurements and line flows is given in equation 3.22. Moreover, the line flows, and hence switch status of the branches can be estimated as given in equation 3.24.

$$\mathrm{z_{en}} = \mathrm{H_{en}} \cdot \mathrm{x_{en}} + \mathrm{e_{en}} \tag{3.22}$$

$$(H^T \cdot H) \cdot \hat{x}_{en} = H_{en}^T \cdot z_{en} \tag{3.23}$$

$$G_{en} \cdot \hat{x}_{en} = t_{en} \tag{3.24}$$

Assume that z_{en} is a vector of zeros. If the G_{en} is non-singular, such that all branch status can be identified uniquely, the state vector, x_{en} will also be a vector of zeros trivially. If G_{en} is singular, i.e., the status of some branches is not uniquely identifiable, then one will encounter zero-pivots during the Cholesky factorization of G_{en}. The presence of those zero-pivots disables factorization. As stated by the incomplete Cholesky factorization, when a zero pivot encountered, it will be replaced by 1, and the corresponding entry of t_{en} vector will be assigned an integer number in increasing order and starting at 1 [30]. At the end of the incomplete Cholesky factorization, an updated non-singular gain matrix, G'_{en} and the updated t'_{en} will be obtained. Equation 3.24 will be solved using G'_{en} and t'_{en}. In the end, the non-zero entries of $\hat{x}_{en}$ reveals the branches whose status cannot be identified uniquely, and hence constitutes a ring in the topology. Algorithm 2 presents the proposed algorithm.

Note that, at this stage, the proposed method aims to determine the branches that form a ring. Those rings are not identified, and identification of each ring is out of the scope of the restoration process. However, the contribution of the proposed DRS method in the IRS is given in Chapter 3.2 as a side contribution of this work.

Algorithm 2 Detection of Ring Structure

Form H matrix and obtain H_{en} by re-ordering
$G_{en} = H_{en}^{T} \cdot H_{en}$
$t'_{en} = zeros(\#states)$
$pivots, G'_{en} = incomplete.cholesky(G_{en})$
$counter = 1$
    for *each pivot* **do**
        if $pivot.value == 0$ **then**
            $\boldsymbol{t'_{en}}(pivot\,.index) = counter$
            counter = counter +1
        end
    end
$\hat{x} = inv(G'_{en}) \cdot t'_{en}$
ring structured branches = corresponding non-zero entries of $\hat{x}$
radial structured branches = corresponding zero entries of $\hat{x}$

3.1.3 Application on Three Bus Sample System

To better illustrate the methodology, the proposed method is employed at a sample system shown in Figure 3.4. The branches and buses are shown in red and black numbers, respectively. Bus 1 is connected to the transmission network and, Bus 8 is connected to the transmission network via a switch.

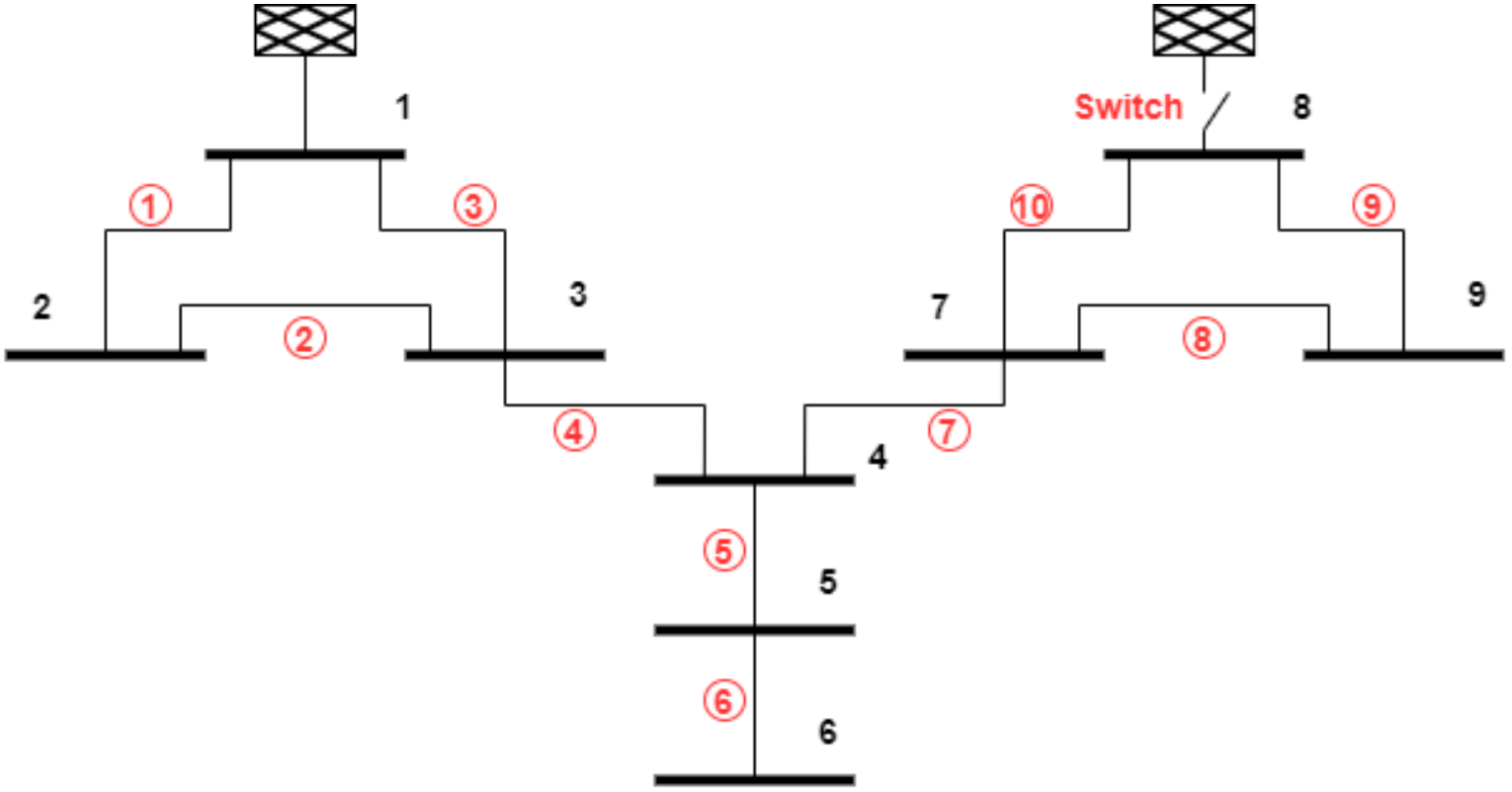

Figure 3.4. Sample 8 bus distribution system

When the switch is open, branches 1,2,3 constitute a ring structure, and branches 8,9,10 constitute another ring structure. If the switch is closed, branches 1,2,3,4,7,8,9,10 are revealed as ring operating branches assuming transmission connections are infinite sources.

Case 1: When the switch is open, the Jacobian matrix, H, corresponding to the current system is given in equation 3.25. As explained in Section 3.1.1, before employing incomplete Cholesky decomposition, strategical ordering is utilized. According to the strategical ordering, row 6 which contains only one non-zero term is replaced by row 1 and column 6 is replaced by column 1. As mentioned earlier, non-zero term at $H'(5,1)$ can be replaced with zero as it is a linear combination of the first row. Thus, row 5 now has only one non-zero term which can be moved to the identity matrix by re-ordering again. In this way, H'' matrix given in equation 3.27 is obtained which is composed of $I\,(2\times 2)$, $0(7\times 2)$, $0(2\times 7)$, $H_{en}\,(7\times 8)$ sub-matrices. $H_{en}\,(7\times 8)$ sub-matrix is highlighted in a green rectangular shape in equation 3.27.

$$H = \begin{array}{c|cccccccccc} & ① & ② & ③ & ④ & ⑤ & ⑥ & ⑦ & ⑧ & ⑨ & ⑩ \\ 1 & -1 & 0 & -1 & 0 & 0 & 0 & 0 & 0 & 0 & 0 \\ 2 & 1 & -1 & 0 & 0 & 0 & 0 & 0 & 0 & 0 & 0 \\ 3 & 0 & 1 & 1 & -1 & 0 & 0 & 0 & 0 & 0 & 0 \\ 4 & 0 & 0 & 0 & 1 & -1 & 0 & -1 & 0 & 0 & 0 \\ 5 & 0 & 0 & 0 & 0 & 1 & -1 & 0 & 0 & 0 & 0 \\ 6 & 0 & 0 & 0 & 0 & 0 & 1 & 0 & 0 & 0 & 0 \\ 7 & 0 & 0 & 0 & 0 & 0 & 0 & 1 & -1 & 0 & -1 \\ 8 & 0 & 0 & 0 & 0 & 0 & 0 & 0 & 0 & -1 & 1 \\ 9 & 0 & 0 & 0 & 0 & 0 & 0 & 0 & 1 & 1 & 0 \end{array} \tag{3.25}$$

H' =

	⑥	②	③	④	⑤	①	⑦	⑧	⑨	⑩
6	1	0	0	0	0	0	0	0	0	0
2	0	-1	0	0	0	1	0	0	0	0
3	0	1	1	-1	0	0	0	0	0	0
4	0	0	0	1	-1	0	-1	0	0	0
5	-1	0	0	0	1	0	0	0	0	0
1	0	0	-1	0	0	-1	0	0	0	0
7	0	0	0	0	0	0	1	-1	0	-1
8	0	0	0	0	0	0	0	0	-1	1
9	0	0	0	0	0	0	0	1	1	0

(3.26)

H'' =

	⑥	⑤	③	④	②	①	⑦	⑧	⑨	⑩
6	1	0	0	0	0	0	0	0	0	0
5	0	1	0	0	0	0	0	0	0	0
3	0	0	1	-1	1	0	0	0	0	0
4	0	-1	0	1	0	0	-1	0	0	0
2	0	0	0	0	-1	1	0	0	0	0
1	0	0	-1	0	0	-1	0	0	0	0
7	0	0	0	0	0	0	1	-1	0	-1
8	0	0	0	0	0	0	0	0	-1	1
9	0	0	0	0	0	0	0	1	1	0

(3.27)

The strategical ordering trivially reveals that branches 5 and 6 are radial structures with no transmission network connections. The remaining components form $G_{en}(8 \times 8) = H_{en}^{T}(8 \times 7) \cdot H_{en}(7 \times 8)$. Incomplete Cholesky factorization explained in Chapter 3.1.2 now can be employed to decompose G_{en}. L'_{en} is obtained by factorizing G_{en} where zero pivots are changed to 1, and t'_{en} vector is modified as shown in equation 3.28-3.29.

L'_{en} =

1.414	0	0	0	0	0	0	0
-0.707	1.225	0	0	0	0	0	0
0.707	-0.408	1.155	0	0	0	0	0
0.707	0.408	-1.155	1	0	0	0	0
0	-0.816	-0.289	0	1.118	0	0	0
0	0	0	0	-0.894	1.095	0	0
0	0	0	0	0	0.913	1.08	0
0	0	0	0	-0.894	0.183	-1.08	1

(3.28)

t'^{T}_{en} =

0	0	0	1	0	0	0	2

(3.29)

Solving equation 3.24 by means of the incomplete Cholesky factorization will yield the $\hat{x}_{en} = inv(G'_{en}) \cdot t'_{en}$. As shown in equation 3.30, the values correspond to Branches 4 and 7 are zero, all other values are non-zero. Branches 5 and 6 are already marked as radial in the strategical ordering process, and as a result, all the radial branches are detected. For the given system, the numeric approach may not be advantageous over graph based search algorithms however, the proposed method provides significant improvement of computational performance for the real-life systems with thousands of buses. The result and comparison of the proposed method are discussed in Chapter 5.

③	④	②	①	⑦	⑧	⑨	⑩

$\hat{x}_{en}$ =

-1	0	1	1	0	-2	2	2

(3.30)

Case 2: When the switch connected to Bus 8 is closed in Figure 3.4, Bus 1 and Bus 8 are assumed to be connected to an infinite feeder. In this configuration, only Branches 5 and 6 are found to be radial. Those branches are detected and removed

in the strategical ordering. The resultant $\hat{x}_{en}$ is full of non-zero values in this case since all the remaining branches constitute a ring.

3.2 Identification of Ring Structure

The proposed DRS method classifies all the buses under two main groups, namely radial structured buses and ring structured buses. In this sub-section, the effect of the proposed DRS method on the identification of the ring structure, IRS, is given. IRS is the process where each ring structure is detected, and the buses forming each ring structure are identified.

Although distribution systems operate in radial structure, there might be ring structured operating buses in practical applications. With the recent developments in renewable resources, the real-time monitoring of the distribution system, hence, identification of the system topology gains significant importance. IRS is a key tool for observability and identifiability analysis of distribution systems.

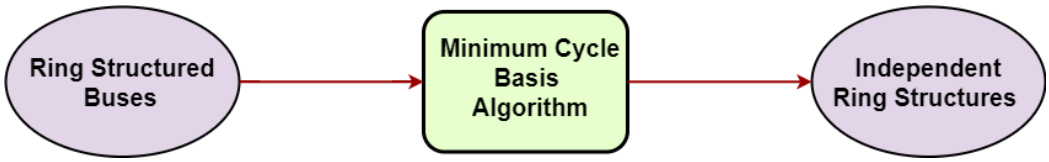

Figure 3.5. Flow diagram of IRS method.

A minimum cycle basis (MCB) algorithm can be used to identify the ring structures in a system as shown in Figure 3.5. MCB is a graph based method that is computationally expensive, and not feasible to be utilized in large distribution systems. Although there are applications that are utilized in the distribution systems with tens of buses, studies based on partitioning of the distribution system with thousands of buses are not present in the literature [13], [35]–[37]. Furthermore, the majority of the buses in a distribution system are radial operating buses. Thus, the

computational performance of the IRS can be significantly improved by utilizing the MCB algorithm to only the ring structured buses where the radial structured buses are eliminated using the proposed DRS method. In other words, instead of utilizing the MCB algorithm to the whole distribution system, it is applied to the ring structured buses which are detected by the proposed DRS method. Since the number of ring structured buses is limited, the computational time is reduced significantly.

The improvement in the performance of IRS is given in Chapter 5.

3.3 Chapter Summary

In this chapter, the detection of ring structure is explained in detail. The aim of the proposed method and its contribution to the distribution system restoration are presented at the beginning of the chapter. Then, the algorithm of the proposed novel partitioning method is provided in Chapter 3.1. The details of strategical ordering, incomplete Cholesky method, and application on a sample system are also given in this chapter. Lastly, although it is not utilized in the proposed methods, the effect of the DRS method in the IRS is given as a side contribution of this thesis. In other words, IRS is not required in the proposed methods, however, identifying the ring structures is required in some applications where it is significantly improved with the proposed DRS method.

CHAPTER 4

SITUATIONAL AWARENESS FOR DISTRIBUTION SYSTEM RESTORATION

In Chapter 3, the proposed partitioning algorithm is presented. The restoration strategy can be developed for ring and radial structured parts separately using the given novel partition method. The proposed method given in Chapter 3 improves the computational time of the decision support mechanism significantly. In this chapter, the improvement in the situational awareness is provided. In Chapter 4 of this thesis, LAV based state estimator and FBPF analysis which are employed in the situational awareness tool are presented.

The situational awareness tool is developed to be utilized in the distribution system restoration. The reason for using those two tools together can be explained using the flow chart given in Figure 4.1. As seen in the figure, once the restoration strategy is determined, the buses are energized according to the restoration action set in real-time operation. The real-time measurements are gathered from the field, and the developed three-phase estimator estimates the system states. Then, FBPF analysis is executed for the whole system to detect any predicted possible violation. Note that initial power injection measurements are load and generation forecasts/profiles which are unreliable. The unreliable power injection measurements are updated for the energized part using state estimation results to improve the accuracy of the injection measurements. Unless there is a violation of electrical constraints in the energized section or a predicted possible violation in the un-energized section, the next action is realized. If there is a violation, firstly electrical constraints are flexed such that the permissible voltage magnitude limits are extended to 0.9 pu and 1.1 pu instead of original limits of 0.95 pu and 1.05 pu. If the obtained voltage magnitude values are still out of the limits, the given action set is marked as infeasible, and an

updated restoration strategy is synthesized considering the infeasible actions. When all the actions in the action set are realized, the restoration is said to be completed.

The state estimation tool makes the situational awareness capable of processing real-time measurements and updating biased power injection measurements whereas the developed power flow algorithm analyzes the system states of the buses to be energized according to the action set in a fast manner.

4.1 Forward/Backward Power Flow

The power flow analysis aims to detect any possible violation of electrical constraints in the distribution system during the restoration. This analysis uses load and generation forecasts/profiles of the buses to be energized. If an action set causes the violation of electrical constraints, firstly the constraints are flexed, and if the violation continues, the action set is marked as infeasible.

Among all the power flow analysis methods, FBPF is the most suitable method to be utilized in the situational awareness tool considering the radial structure and high R/X ratio [17]–[19].

Forward Backward Power Flow (FBPF) algorithm sets the initial values of the bus voltage magnitudes as $1pu$ and bus voltage phase angles as $0°$. The algorithm is an iterative process where two consecutive steps, namely backward sweep and forward sweep are executed in each iteration. In the backward sweep, the current flows are calculated using complex power injections and bus voltage vectors. Then, in the forward sweep, the voltage vector of each bus is updated using impedance values and current flows of the lines. While current flows are calculated starting from the leaf buses toward the slack bus in the backward sweep, voltage vectors of the buses are updated in the forward sweep from the slack bus to leaf buses.

The current injections of the buses are calculated using equation 4.1. The lower case k denotes the number of iteration throughout the FBPF algorithm.

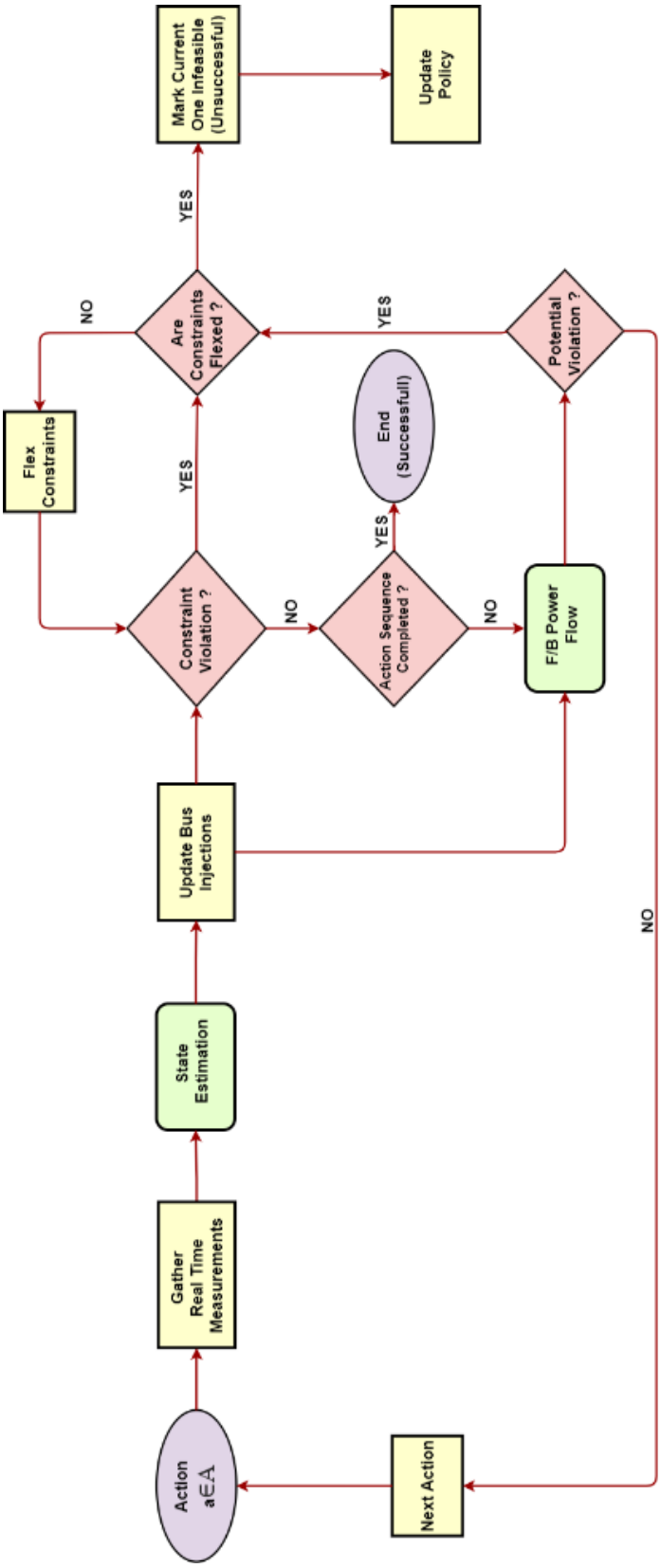

Figure 4.1. Flow diagram of situational awareness tool

$$\boldsymbol{I_{bus}}[k] = \left(\frac{\boldsymbol{S_{bus}}}{\boldsymbol{V_{bus}}[k]}\right)^{*} \tag{4.1}$$

where,

$\boldsymbol{S_{bus}}$: complex power injections of the buses $(n \times 1)$

$\boldsymbol{V_{bus}}[k]$: bus voltage vectors of the buses at iteration k $(n \times 1)$

$\boldsymbol{I_{bus}}[k]$: current injections of the buses at iteration k $(n \times 1)$

n : number of the buses

In the forward sweep of the algorithm, branch current flow vector, I_{branch}, is required. To calculate I_{branch}, Bus Injection to Bus Current (BIBC) matrix should be formed. BIBC matrix will be formed once for the given topology, will not be updated at each iteration. The most straightforward method to obtain the BIBC matrix is using the bus branch incidence matrix, A. While the rows of A represent the branch flows, each column corresponds to a bus. The inverse transpose of A matrix yields the BIBC matrix if the column corresponds to the slack bus is removed. Thus, the relation between bus current injections and branch current flows can be seen in equation 4.2.

$$\boldsymbol{I_{branch}} = \boldsymbol{BIBC} * \boldsymbol{I_{bus}} \tag{4.2}$$

Once the branch current flows are calculated, the backward sweep is completed, and the forward sweep starts. The bus voltages are updated in the forward sweep using impedance values and I_{branch} vector as shown in equation 4.3. The impedance values of the lines are represented inside a diagonal matrix, namely Z_{diag}.

$$\boldsymbol{V_{bus}}[k+1] = \boldsymbol{V_{bus}}[k] - \boldsymbol{Z_{diag}} * \boldsymbol{I_{branch}}[\mathrm{k}] \tag{4.3}$$

Once the error is smaller than the predefined tolerance value, the algorithm is said to be converged. The error value is computed as $\max|V_{bus}[k+1] - V_{bus}[k]|$. The overall FBPF algorithm is given in Algorithm 3.

Algorithm 3 FBPF BIBC Matrix Method

1: Form system connectivity matrix and calculate **BIBC**
2: Form diagonal impedance matrix, $\boldsymbol{Z_{diag}}$
3: determine flat start values, $\boldsymbol{V_{bus}}[0]$
4: determine predefined tolerance value, ϵ
6: $k = 0,\ \boldsymbol{error} = 100$
7: **while** $\max|\boldsymbol{error}| > \epsilon$
8: $\boldsymbol{I_{bus}}[k] = \left(\frac{\boldsymbol{S_{bus}}}{\boldsymbol{V_{bus}}[k]}\right)^*$
9: $\boldsymbol{I_{branch}}[k] = \boldsymbol{BIBC} * \boldsymbol{I_{bus}}[k]$
10: $\boldsymbol{V_{bus}}[k+1] = \boldsymbol{V_{bus}}[k] - \boldsymbol{Z_{diag}} * \boldsymbol{I_{branch}}[k]$
11: $\boldsymbol{error} = \boldsymbol{V_{bus}}[k+1] - \boldsymbol{V_{bus}}[k]$
12: k = k+1
15: **end**
16: bus voltage vector = $\boldsymbol{V_{bus}}[k+1]$

The FBPF algorithm is employed in a six-bus sample system to illustrate the method. The sample system is given in Figure 4.2 where buses are indicated in black, and branches are shown in red.

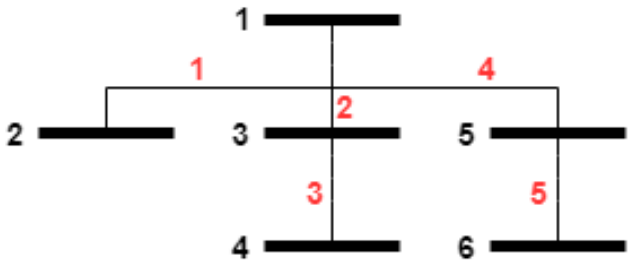

Figure 4.2. Six-bus sample system

The construction of the BIBC matrix is given in equations 4.4-4.6. As explained earlier, the bus branch incidence matrix, A, is utilized to obtain the BIBC matrix. The A matrix for the given sample system is shown in equation 4.4. A' matrix is obtained by removing the column representing the slack bus. $BIBC'$ matrix can be obtained by taking the inverse of A'^{T} as shown in equation 4.5. Finally, $BIBC$ matrix is finalized by inserting a zero column to represent the slack bus.

$$\boldsymbol{A} = \begin{bmatrix} -1 & 1 & 0 & 0 & 0 & 0 \\ -1 & 0 & 1 & 0 & 0 & 0 \\ 0 & 0 & -1 & 1 & 0 & 0 \\ -1 & 0 & 0 & 0 & 1 & 0 \\ 0 & 0 & 0 & 0 & -1 & 1 \end{bmatrix} \tag{4.4}$$

$$\boldsymbol{BIBC' = inv(A'^{T})} \tag{4.5}$$

$$\boldsymbol{BIBC} = \begin{bmatrix} 0 & 1 & 0 & 0 & 0 & 0 \\ 0 & 0 & 1 & 1 & 0 & 0 \\ 0 & 0 & 0 & 1 & 0 & 0 \\ 0 & 0 & 0 & 0 & 1 & 1 \\ 0 & 0 & 0 & 0 & 0 & 1 \end{bmatrix} \tag{4.6}$$

Z_{diag} matrix is formed by inserting the impedance value of i^{th} branch to the $Z_{diag}(i,i)$. Once the $BIBC$ and Z_{diag} matrices are obtained, the iterative procedure starts with flat start values of the bus voltages. In the backward sweep, the current

injection vector at iteration k is obtained using equation 4.7. I_{branch} vector is calculated using $BIBC$ in equation 4.8.

$$\boldsymbol{I_{bus}}[k]_{\boldsymbol{6x1}} = \begin{bmatrix} \frac{S_{bus,1}}{V_{bus}[k]_1} \\ \frac{S_{bus,2}}{V_{bus}[k]_2} \\ \vdots \\ \frac{S_{bus,6}}{V_{bus}[k]_6} \end{bmatrix} \tag{4.7}$$

$$\boldsymbol{I_{branch}}[k] = \boldsymbol{BIBC} * \boldsymbol{I_{bus}}[k] \tag{4.8}$$

The forward sweep is executed by updating the voltage vector of each bus as shown in equation 4.9.

$$\begin{bmatrix} V_{bus}[k+1]_1 \\ V_{bus}[k+1]_2 \\ \vdots \\ V_{bus}[k+1]_6 \end{bmatrix} = \begin{bmatrix} V_{bus}[k]_1 \\ V_{bus}[k]_2 \\ \vdots \\ V_{bus}[k]_6 \end{bmatrix} - \begin{bmatrix} Z_1 & \cdots & 0 \\ \vdots & \ddots & \vdots \\ 0 & \cdots & Z_5 \end{bmatrix} * \boldsymbol{I_{branch}}[k] \tag{4.9}$$

where Z_1 is the impedance value of branch 1 shown in Figure 4.2.

4.2 State Estimation for Distribution System

There are various power system state estimation methods in the literature [30]. State estimation is mostly utilized in the transmission system where the system is fully observable.

Redundant measurement devices and SCADA system make the transmission network observable whereas the distribution system suffers from the lack of measurement. However, with the popularization of new technologies such as renewable resources and electrical vehicles, the necessity of real-time monitoring at

the distribution level became comprehensible. Therefore, the number of measurements in the distribution network is increased in the recent decade which makes state estimation application feasible in the distribution networks.

Transmission system state estimation employs the positive sequence model of the system considering balanced structure and load profile. On the other hand, even in the normal operation, distribution systems may be unbalanced due to lack of transposition, unbalanced loads, and high R/X ratio [28]. Moreover, the developed estimator is expected to be employed in the post-disaster distribution systems where unbalanced conditions are effective on the solution. Therefore, in this study, the three-phase model of the distribution system is required for the sake of estimation accuracy [29].

WLS is the most common solution method to be utilized in the transmission system state estimation thanks to its computational performance [38]. However, the WLS method is vulnerable against bad data, thus bad data analysis is required, and can be utilized if measurement redundancy is high enough. In the distribution system, pseudo measurements are placed to ensure system observability. The limited number of measurements and inaccuracy of the pseudo measurements make the WLS method vulnerable against bad data in the distribution system. Especially, after a disaster, the accuracy of the pseudo measurements is highly unreliable. The use of LAV estimation, on the other hand, provides an automatic rejection of the bad data or inaccurate pseudo measurement. The LAV estimator aims to obtain a set of measurements minimizing the least absolute values of the measurement residuals.

As a result, LAV based method using the three-phase model is selected as an estimation method. Furthermore, the performance of the LAV estimator is improved by partially linearizing the measurement function. Comparison of computational performances of LAV and WLS estimators is given the Chapter 5 with a detailed discussion to justify the proposed selection. Also, the impact of partial linearization in the LAV estimation is validated in Chapter 5 with computational performance results.

4.3 The Three-Phase LAV State Estimation

In this subsection, the proposed three-phase LAV estimation will be explained. The states of the proposed estimation are three-phase bus voltage magnitudes and three-phase bus voltage phase angles. Moreover, available real-time measurements in the distribution network are three-phase bus voltage magnitudes, three-phase real/reactive power injection measurements and three-phase current magnitude measurements. The basic assumptions providing the mathematical model construction are given in the background section.

The measurement model for the estimator is given in equation 4.10.

$$z = \begin{bmatrix} h_1(x_1, x_2, \dots, x_n) \\ h_2(x_1, x_2, \dots, x_n) \\ \vdots \\ h_m(x_1, x_2, \dots, x_n) \end{bmatrix} + e = h(x) + e \qquad (4.10)$$

where;

$h_i(x)$: the function relating measurement i to the state vector x,

z : the set of measurement

e : the measurement error vector

x : the system states vector where the states are three-phase bus voltage magnitudes and phase angles

In three-phase configuration;

$$z = \begin{bmatrix} z_1^a & z_1^b & z_1^c & \dots & z_i^a & z_i^b & z_i^c & \dots & z_m^a & z_m^b & z_m^c \end{bmatrix}^T$$

$$x = \begin{bmatrix} \theta_1^{3ph} & \theta_2^{3ph} & \dots & \theta_n^{3ph} & V_1^{3ph} & V_2^{3ph} & \dots & V_n^{3ph} \end{bmatrix}^T$$

where,

m : number of measurements per phase

n : number of buses

$V_i^{3ph} = \begin{bmatrix} V_i^a & V_i^b & V_i^c \end{bmatrix}^T$

$\theta_i^{3ph} = \begin{bmatrix} \theta_i^a & \theta_i^b & \theta_i^c \end{bmatrix}^T$

z_i^l : the measured value of i^{th} measurement for ph-l

V_i^l : bus voltage magnitude at bus-i for phase-l

θ_i^l : bus voltage angle at bus-i for phase-l

Note that number of total measurements is $3m$ considering m is the number of measurements per phase. Similarly, the number of states is $6n$ where $3n$ of the states are three-phase bus voltage magnitudes and $3n$ of the states are three-phase bus voltage phase angles assuming all bus voltages and angles are states.

The objective function of the LAV based estimation is given in equation 4.11.

$$\begin{aligned} &\text{minimize} \quad \sum_{i=1}^{3m} |r_i| \\ &\text{subject to} \quad z_i = h_i(x) + r_i\,, \qquad 1 \le i \le 3m \end{aligned} \tag{4.11}$$

where, r_i is the residual of i^{th} measurement corresponding to the difference between the real value of the measurement and the estimated value of the measurement, i.e., $r_i = z_i - h(\hat{x}_i)$. Using the first-order approximation of $h_i(x^0)$ around of x^0, the problem can be rewritten as linear programming (LP) problem. The problem is given as a standard LP problem in equation 4.12.

$$\mathrm{J}(\mathrm{x}^{\mathrm{k}}) = \sum_{i=1}^{3m} (u_i^k + v_i^k) \tag{4.12}$$

where;

$u^k - v^k = z - h(x^k) - H(x^k) \cdot \Delta x = \Delta z^k - H(x^k) \cdot \Delta x^k$

In equation 4.12, $(u^k + v^k)$ term corresponds to the measurement residual vector at iteration k. Dropping the superscript k for the simplicity of the notation, the problem can be formulated as shown in equation 4.13.

$$\begin{aligned} \text{minimize} \quad & \sum_{i=1}^{3m} (u_i + v_i) \\ \text{subject to} \quad & H \cdot \Delta x_u - H \cdot \Delta x_v + u - v = \Delta z \\ & \Delta x_u, \Delta x_v, u, v \geq 0 \end{aligned} \tag{4.13}$$

where;

$\Delta x = \Delta x_u - \Delta x_v$

Lastly, the LP problem can be written in the compact form as given in equation 4.14.

$$\begin{aligned} \text{minimize} \quad & c^T \cdot Y \\ \text{subject to} \quad & A \cdot Y = b \\ & Y \geq 0 \end{aligned} \tag{4.14}$$

where,

$c^T = [0_{6n}, 0_{6n}, 1_{3m}, 1_{3m}]$,

0_{6n} : a zero vector of order $6n$,

1_{3m} : a vector of order $3m$, where all the entries are 1,

$b = \Delta z$,

$Y^T = [\Delta x_u^T, \Delta x_v^T, u^T, v^T]$,

$A = [H, -H, I_{3m}, -I_{3m}]$,

I_m : an identity matrix of order $3m$.

The determination of the initial values of the states requires additional effort due to current flow measurements. The initial values of the states are conventionally selected as flat start values, i.e., $V = 1\ pu$ and $\theta = 0°$. However, flat start values make the current magnitude calculation undefined due to zero value in the denominator. Therefore, manipulated flat start values are utilized to initialize the state vector where θ values are randomly assigned between $-0.01°\ and\ 0.01°$.

At each iteration, measurement values are estimated using the current state vector. Similarly, H matrix is formed in each iteration using the current state vector. Then, the LP problem given in equation 4.14 is solved to obtain Δx. As a result of the LP problem solution, Δx is obtained as shown in equation 4.15, and the states are updated as shown in equation 4.16.

$$\Delta x = \left[\Delta\theta_1^{3ph}\ \ \Delta\theta_2^{3ph} \ldots\ \Delta\theta_n^{3ph}\ \ \Delta V_1^{3ph}\ \ \Delta V_2^{3ph} \ldots\ \Delta V_n^{3ph}\right]^T \qquad (4.15)$$

$$x^{k+1} = x^k + \Delta x^k \qquad (4.16)$$

The iterative procedure is converged if $\max|\Delta x^k| < \epsilon$ where ϵ is the predefined error threshold value.

To derive the measurement Jacobian matrix, H, firstly the measurement function, $h(x^k)$, should be obtained for each measurement type. The relation of the measurements with respect to the states is given in equations 4.17-4.19.

$$P_i^{ph} = V_i^{ph} * \sum_{l=1}^{3} \sum_{j \epsilon N_i} V_j^{l} * (G_{ij}^{ph,l} cos(\theta_i^{ph} - \theta_j^{l}) + B_{ij}^{ph,l} sin(\theta_i^{ph} - \theta_j^{l})) \quad (4.17)$$

$$Q_i^{ph} = V_i^{ph} * \sum_{l=1}^{3} \sum_{j \epsilon N_i} V_j^{l} * \left(G_{ij}^{ph,l} sin(\theta_i^{ph} - \theta_j^{l}\right) - B_{ij}^{ph,l} cos(\theta_i^{ph} - \theta_j^{l})) \quad (4.18)$$

$$I_{ij}^{ph} = \sum_{l=1}^{3} \left[V_i^{ph}\left(cos\theta_i^{l} + jsin\theta_i^{l}\right) - V_i^{ph}\left(cos\theta_i^{l} + jsin\theta_i^{l}\right)\right] * Y_{ij}^{ph,l} \quad (4.19)$$

where,

$G_{ij}^{ph,l}$: the corresponding element of conductance matrix for bus-i phase-ph and bus-j phase-l

$B_{ij}^{ph,l}$: the corresponding element of susceptance matrix for bus-i phase-ph and bus-j phase-l

P_i^{ph} : real power injection measurement at bus-i for phase-ph

Q_i^{ph} : reactive power injection measurement at bus-i for phase-ph

I_{ij}^{ph} : magnitude of current flow between bus-i and bus-j for phase--ph

Conductance matrix (G) and susceptance matrix (B) are obtained by forming the bus admittance matrix (Y_{bus}). To be able to form Y_{bus} matrix, three-phase impedance matrix of the lines should be obtained.

In a two-bus system, the structure of the three-phase bus impedance matrix (Z) is shown in equation 4.20. In the equation, elements of the matrix model the self-impedance and mutual impedance values between bus-i and bus-j. Furthermore, Y_{bus} for the two bus system is formed using the inverse of Z matrix in equation 4.21.

$$Z_{ij} = \begin{bmatrix} Z^{aa} & Z^{ab} & Z^{ac} \\ Z^{ba} & Z^{bb} & Z^{bc} \\ Z^{ca} & Z^{cb} & Z^{cc} \end{bmatrix} \tag{4.20}$$

$$Y_{bus} = \begin{bmatrix} {Z_{ij}}^{-1}{}_{3x3} & -{Z_{ij}}^{-1}{}_{3x3} \\ -{Z_{ij}}^{-1}{}_{3x3} & {Z_{ij}}^{-1}{}_{3x3} \end{bmatrix} \tag{4.21}$$

Z_{ij} : impedance matrix corresponding to the line between bus-i and bus-j

Z^{aa} : self-impedance value of the line between bus-i and bus-j for phase-a

Z^{ba} : mutual-impedance value of the line between bus-i and bus-j for phase-a and phase-b

Y_{bus} : bus admittance matrix

The impedance information in this work is provided as a sequence impedance matrix (Z_{012}). Z_{012} represents the impedance values of positive, negative, and zero sequences while the state estimation is designed to process the phase impedance matrix (Z). To transform the sequence matrix into the phase impedance matrix, a simple matrix multiplication shown in equation 4.22 is used. Thus, for each cable type, firstly Z_{012} is obtained, and then it is transformed into Z.

$$Z = A_s \cdot Z_{012} \cdot A_s^{-1} \tag{4.22}$$

where;

$$A_s = \begin{bmatrix} 1 & 1 & 1 \\ 1 & a_s^2 & a_s \\ 1 & a_s & a_s^2 \end{bmatrix}, \qquad {A_s}^{-1} = \frac{1}{3} \cdot \begin{bmatrix} 1 & 1 & 1 \\ 1 & a_s & a_s^2 \\ 1 & a_s^2 & a_s \end{bmatrix}$$

$a_s = 1.0\angle 120°$

As shown in equation 4.21, the size of the Y_{bus} will be $(n \times 3) \times (n \times 3)$. The structure of Y_{bus} for a n bus system is given in equation 4.23.

$$Y_{bus} = \begin{bmatrix} Y_{11}^{aa} & Y_{11}^{ab} & Y_{11}^{ac} & \cdots & Y_{1n}^{aa} & Y_{1n}^{ab} & Y_{1n}^{ac} \\ Y_{11}^{ba} & Y_{11}^{bb} & Y_{11}^{bc} & \cdots & Y_{1n}^{ba} & Y_{1n}^{bb} & Y_{1n}^{bc} \\ Y_{11}^{ca} & Y_{11}^{cb} & Y_{11}^{cc} & \cdots & Y_{1n}^{ca} & Y_{1n}^{cb} & Y_{1n}^{cc} \\ \vdots & \vdots & \vdots & \ddots & \vdots & \vdots & \vdots \\ Y_{n1}^{aa} & Y_{n1}^{ab} & Y_{n1}^{ac} & \cdots & Y_{nn}^{aa} & Y_{nn}^{ab} & Y_{nn}^{ac} \\ Y_{n1}^{ba} & Y_{n1}^{bb} & Y_{n1}^{bc} & \cdots & Y_{nn}^{ba} & Y_{nn}^{bb} & Y_{nn}^{bc} \\ Y_{n1}^{ca} & Y_{n1}^{cb} & Y_{n1}^{cc} & \cdots & Y_{nn}^{ca} & Y_{nn}^{cb} & Y_{nn}^{cc} \end{bmatrix} \quad (4.23)$$

Knowing $Y_{bus} = (G + j\,B)$, G and B matrices can be obtained once the three-phase Y_{bus} is formed. By substituting conductance, susceptance and state values into the equations 4.17 - 4.19, the non-linear relation, $h(.)$, between states and measurements can be calculated.

To solve the state estimation problem, the Jacobian matrix, H, is also required. H matrix includes derivate of $h(.)$ with respect to each state variable. While the columns of the H matrix represent the states to be estimated, each row of the H matrix corresponds to a measurement. Thus, the size of the H matrix is $(3 \times m) \times (6 \times n)$. The structure of the H matrix is given in equation 4.24.

$$\boldsymbol{H} = \begin{bmatrix} \frac{\partial P_i^{ph}}{\partial \theta_i^{A}} & \frac{\partial P_i^{ph}}{\partial \theta_i^{B}} & \frac{\partial P_i^{ph}}{\partial \theta_i^{C}} & \frac{\partial P_i^{ph}}{\partial V_i^{A}} & \frac{\partial P_i^{ph}}{\partial V_i^{B}} & \frac{\partial P_i^{ph}}{\partial V_i^{C}} \\ \frac{\partial Q_i^{ph}}{\partial \theta_i^{A}} & \frac{\partial Q_i^{ph}}{\partial \theta_i^{B}} & \frac{\partial Q_i^{ph}}{\partial \theta_i^{C}} & \frac{\partial Q_i^{ph}}{\partial V_i^{A}} & \frac{\partial Q^{ph}}{\partial V_i^{B}} & \frac{\partial Q_i^{ph}}{\partial V_i^{C}} \\ \frac{\partial I_i^{ph}}{\partial \theta_i^{A}} & \frac{\partial I_i^{ph}}{\partial \theta_i^{B}} & \frac{\partial I_i^{ph}}{\partial \theta_i^{C}} & \frac{\partial I_i^{ph}}{\partial V_i^{A}} & \frac{\partial I_i^{ph}}{\partial V_i^{B}} & \frac{\partial I_i^{ph}}{\partial V_i^{C}} \end{bmatrix} \quad (4.24)$$

The formulations of the elements of the H matrix are given in equations A.1- A.4 in Appendix A. The input files of the estimator are Common Format Data (CDF) file which contains the system connectivity information, and the measurement file which includes the measurement types and values. The input values are processed, and all the values are converted into pu units. In Appendix B, a sample system and its input files are given. In Figure B.1, the sample 3-bus system is given. While Figure B.2

shows the CDF file of the corresponding system, Figure B.3 shows the measurement file for the given system. The overall algorithm of the three-phase state estimation is given in Algorithm 4.

Algorithm 4 Three-Phase LAV Estimation

1: Form Y_{bus} matrix and z vector using input files
2: determine manipulated flat start values, x^0
3: determine predefined threshold value, ϵ
4: $k = 0,\ \Delta x^0 = 100$
5: ***while*** $\max|\Delta x^k| > \epsilon$
6: $h_{estimated} = h(x^k)$
7: $H = form.Hmatrix(x^k)$
8: $c^T = [0_{6n}, 0_{6n}, 1_{3m}, 1_{3m}]$
9: $A = [H, -H, I_{3m}, -I_{3m}]$
10: $b = z - h_{estimated}$
11: $Y = [0_{6n+3m}\ \ 0_{6n+3m}]$
12: $\Delta x^k = simplex.solver(c, A, b, Y)$
13: $x^{k+1} = x^k + \Delta x^k$
14: $k = k + 1$
15: ***end***
16: estimated states = x^{k+1}

4.3.1 Performance Improvement of The Estimator

Although the LAV estimator is known to be robust, its computational time is greater compared to the WLS estimator [30]. The selection of the estimator is discussed in Chapter 4.2 in detail. Considering the estimator will be executed multiple times,

improving computational time is significant. To reduce the computational time of the LAV estimator, the measurement function is simplified using valid assumptions.

Fully linearization of the measurement functions is possible by inserting a significant number of new states which do not reduce the computational time [39], [40].

Using the domain-specific advantage of the distribution system, the given measurement formulations are partially linearized to obtain better computational performance. The bus voltage phase angle difference between incident buses is small enough. Thus small-angle approximation can be utilized as shown in equations 4.25 – 4.30. The validation of this simplification is given in Chapter 5.

$$sin\left(\theta_A^i - \theta_A^j\right) = \theta_A^i - \theta_A^j \tag{4.25}$$

$$cos\left(\theta_A^i - \theta_A^j\right) = 1 \tag{4.26}$$

$$sin\left(\theta_A^i - \theta_B^j\right) = cos\left(\frac{2\pi}{3}\right) \cdot \left(\theta_A^i - \theta_B^j + \frac{2\pi}{3}\right) + sin\left(\frac{2\pi}{3}\right) \tag{4.27}$$

$$cos\left(\theta_A^i - \theta_B^j\right) = cos\left(\frac{2\pi}{3}\right) - sin\left(\frac{2\pi}{3}\right) \cdot \left(\theta_A^i - \theta_B^j + \frac{2\pi}{3}\right) \tag{4.28}$$

$$sin\left(\theta_A^i - \theta_C^j\right) = cos\left(\frac{2\pi}{3}\right) \cdot \left(\theta_A^i - \theta_C^j + \frac{2\pi}{3}\right) - sin\left(\frac{2\pi}{3}\right) \tag{4.29}$$

$$cos\left(\theta_A^i - \theta_C^j\right) = cos\left(\frac{2\pi}{3}\right) + sin\left(\frac{2\pi}{3}\right) \cdot \left(\theta_A^i - \theta_C^j + \frac{2\pi}{3}\right) \tag{4.30}$$

By substituting the simplified terms in the measurement functions, the updated measurement functions can be obtained. In equations 4.31-4.32, only the updated measurement functions for phase-A are given for simplicity, however, the philosophy for phase B and C are the same.

$$P_i^A = V_i^A * \sum_{j\epsilon N_i} V_j^A * (G_{ij}^{A,A} + B_{ij}^{A,A}(\theta_i^A - \theta_j^A)) +$$
$$\sum_{j\epsilon N_i} V_j^B \left(G_{ij}^{A,B} \left(cos\left(\frac{2\pi}{3}\right) - sin\left(\frac{2\pi}{3}\right) \cdot \left(\theta_A^i - \theta_B^j + \frac{2\pi}{3}\right)\right) + \right.$$
$$\left. B_{ij}^{A,B} \left(cos\left(\frac{2\pi}{3}\right) \cdot \left(\theta_A^i - \theta_B^j + \frac{2\pi}{3}\right) + sin\left(\frac{2\pi}{3}\right)\right)\right) + \sum_{j\epsilon N_i} V_j^C * \quad (4.31)$$
$$(G_{ij}^{A,C} \left(cos\left(\frac{2\pi}{3}\right) + sin\left(\frac{2\pi}{3}\right) \cdot \left(\theta_A^i - \theta_C^j + \frac{2\pi}{3}\right)\right) + B_{ij}^{A,C} \left(cos\left(\frac{2\pi}{3}\right) \cdot$$
$$\left(\theta_A^i - \theta_C^j + \frac{2\pi}{3}\right) - sin\left(\frac{2\pi}{3}\right)\right))$$
$$Q_i^A = V_i^A * \sum_{j\epsilon N_i} V_j^A * \left(G_{ij}^{A,A}(\theta_i^A - \theta_j^A) - B_{ij}^{A,A}\right) + \sum_{j\epsilon N_i} V_j^B *$$
$$\left(G_{ij}^{A,B} \left(cos\left(\frac{2\pi}{3}\right) \cdot \left(\theta_A^i - \theta_B^j + \frac{2\pi}{3}\right) + sin\left(\frac{2\pi}{3}\right)\right) - B_{ij}^{A,B} \left(cos\left(\frac{2\pi}{3}\right) - \right.$$
$$\left. sin\left(\frac{2\pi}{3}\right) \cdot \left(\theta_A^i - \theta_B^j + \frac{2\pi}{3}\right)\right)\right) + \sum_{j\epsilon N_i} V_j^C * \left(G_{ij}^{A,C} \left(cos\left(\frac{2\pi}{3}\right) \cdot \right. \quad (4.32)$$
$$\left(\theta_A^i - \theta_C^j + \frac{2\pi}{3}\right) - sin\left(\frac{2\pi}{3}\right)\right) - B_{ij}^{A,C} \left(cos\left(\frac{2\pi}{3}\right) + sin\left(\frac{2\pi}{3}\right) \cdot$$
$$\left.\left.\left(\theta_A^i - \theta_C^j + \frac{2\pi}{3}\right)\right)\right)$$

The simplification in the measurement functions affects the accuracy of the estimation while reducing the computational time. The effect of this simplification is discussed in Chapter 5. It is revealed that while the improvement in the computational time is significant, the accuracy of the estimator with the simplified formulation is comparable with the original LAV estimator.

4.4 Chapter Summary

In this chapter, situational awareness for the distribution system restoration is given. The mechanism of the situational awareness tool is explained using the flow chart given in Figure 4.1. As mentioned, both FBPF analysis and state estimator are essential in the restoration process. The details of the FBPF algorithm are presented

in the first sub-chapter of this chapter. Since the selection of estimator is critical, the reasoning behind the LAV based estimation is discussed in Chapter 4.2. Although the basic concept of state estimation in power systems is given in background information, the developed state estimator is three-phase and computationally improved. While the mathematical basis of the estimator is revealed in Chapter 4.3, the partially linearized measurement function to improve the computational performance is given in Chapter 4.3.1.

To sum up, the combination of state estimator and FBPF analysis is the proposed method to provide the situational awareness during the restoration of a distribution system. While state estimation is capable of processing three-phase real-time measurements to estimate the states of the energized part of the system, FBPF analysis conducts a feasibility analysis for the given restoration actions.

CHAPTER 5

VALIDATION OF THE METHOD & TEST RESULTS

In Chapter 4, the proposed situational awareness tool is presented. The overall mechanism is developed to monitor the power distribution system in real-time and detect any infeasible action set causing the violation of electrical constraints during the restoration. In Chapter 4, it is aimed to develop the structure given in Figure 4.1 in an efficient and accurate manner. The computational performance of the state estimator is improved without the loss of accuracy significantly by the partially linearized measurement function. Furthermore, the results of the estimator are used to update the unreliable forecasts and profiles for the energized part of the system to improve the accuracy of the power flow analysis. Initially, if there is a violation of electrical constraints, the permissible limits of the voltage magnitude and power flow magnitudes are flexed. If the violation continues, the given restoration strategy, action set, is marked as infeasible. In that case, a new restoration strategy is requested to be able to continue real-time operation in the field.

In this chapter, all of the proposed methods are validated with proper test cases. Initially, the efficiency of the DRS method is given by revealing the computational time performances of the restoration decision process considering (i) whole system topology and (ii) radial/ring structures separately. Moreover, the superiority of the incomplete Cholesky factorization in the proposed DRS method is also presented. As mentioned earlier, although IRS is not included in the restoration process, the improvement in the IRS is validated by identifying the ring structures of a system with/without employing the DRS method. The tools that are employed in situational awareness are also analyzed in this chapter. The computational time performances and accuracy results of both tools are given. The selection of the estimation method is justified by utilizing different types of estimators in sample systems. The improvement in the estimator performance by partial linearization is also validated.

To evaluate the accuracy of the proposed tools, well-known metrics are utilized, e.g., MSE, MAPE, etc. Lastly, the test environments for each case are presented throughout the chapter.

5.1 Test Results for the Partition of Distribution System

Case 1: In the detection of ring structure method, it is stated that incomplete Cholesky factorization is utilized to G_{en} and the state vector is calculated using the equation $\hat{x}_{en} = ((L'_{en} \cdot L'_{en})^{-1} \cdot t'_{en})$ instead of taking row reduced echelon form of the matrix. In this case, the computational performances of those two methods are compared in Figure 5.1. As shown in the figure, the incomplete Cholesky factorization is superior compared to the taking row reduced echelon form when the size of the matrix is increased while the sparsity ratio is kept constant. As the figure is given in the logarithmic scale, the difference between the performance of those two methods increases significantly as the matrix size increases. The given test is conducted on an Intel i7, 8GB computer using MATLAB environment.

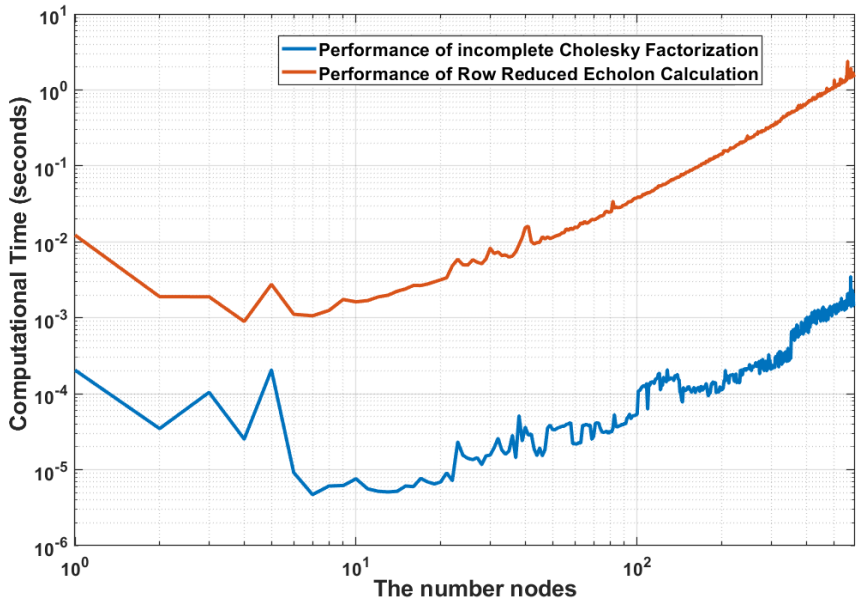

Figure 5.1. The computational performance comparison of (i) Cholesky factorization and (ii) taking row reduced echelon form

Case 2: In this case, a real-life distribution system is partitioned using the proposed DRS method. The results of the partitioning are given in Table 5.1. As stated in the motivation of the method, the method is efficient and makes the restoration process feasible in large-sized distribution systems. To test the computational time, 2xIntel(R) Xeon(R) CPU E5-2650 v4 @ 2.20GHz with 64GB RAM hardware setup is used.

Table 5.1 8477 Bus Distribution System Results

Property	*Value*
Number of Buses	8477
Number of Branches	8498
Computational Time of the DRS method	59.25 sec

Case 3: The partitioning method is proposed to reduce the computational time of the restoration decision process. In this case, the computational time performances of the decision process are given with/without using the proposed partitioning method. To test the computational time, 2xIntel(R) Xeon(R) CPU E5-2650 v4 @ 2.20GHz with 64GB RAM hardware setup is used.

Table 5.2 Comparison of the computational performance of restoration decision process (i) without using the partitioning method, and (ii) using the partitioning method

Performance of the Restoration Decision Process	*Without partitioning*	*With partitioning*
123 Bus System with %10 Radial Structure	356.851 sec	347.727 sec
123 Bus System with %50 Radial Structure	18.185 sec	9.602 sec
123 Bus System with %90 Radial Structure	3.908 sec	2.26 sec

As seen in Table 5.2, the computational performance test is conducted using a 123 bus system with modified density of radial structures. It is expected to observe more improvement in the restoration as the ratio of radial structures increases. When %10 of the branches are radial structured, the partitioning does not contribute a significant improvement to the restoration process since the majority of the branches are ring structured, and they maintain the combinatorial restoration possibilities. However, when the %50 of the branches are radial, the computational time is almost halved as the ring/radial structures are processed separately. In the %90 radial structure case, since the possible restoration paths are already limited due to a few ring structured branches, the improvement in the computational performance cannot be observed clearly.

Case 4: In this case, the performance improvement of the IRS method is shown. The computational time of identifying independent ring structures and its elements using graph based method, e.g., Minimum Cycle Basis (MCB) method is compared with the computational time of Ring system Detection and Extraction (RDE) followed by MCB. To test the computational time, 2xIntel(R) Xeon(R) CPU E5-2650 v4 @ 2.20GHz with 64GB RAM hardware setup is used. 5 Monte-Carlo simulations are run, and their average is given as a result. The standard deviation of the simulation results is less than %3.

For the test, various number of buses in a real-life distribution system is employed. Figure 5.2 shows the difference of computational time performances in the logarithmic scale for (i) MCB is utilized to identify the ring structures for the whole system and (ii) radial structure is detected and extracted from the system, and then MCB is utilized. As seen in the figure, the proposed method is superior compared to the conventional graph based method. Elimination of the radial structure simplifies the computational complexity and makes the IRS method efficient for large-sized distribution systems using MCB. As stated in the motivation of the method, MCB only method can not converge in a reasonable time when the size of the system is

around ten thousand. Considering large-sized distribution systems, the partitioning method plays a significant role in the topology analysis.

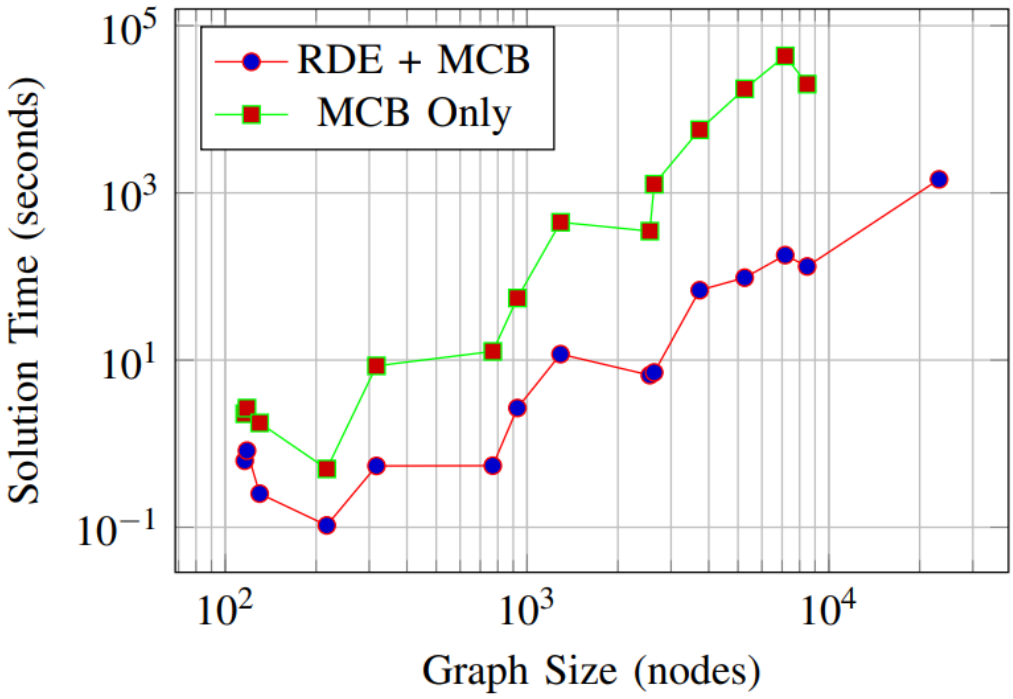

Figure 5.2. Performance of IRS using (i) MCB only, and (ii) RDE followed by MCB

5.2 Test Results for Situational Awareness

Case 1: The performance of the FBPF method is evaluated by comparing the result of the power flow analysis with the result of the simulation tool. In 12 bus system, the MSE of the FBPF method is revealed as $\mathbf{6.0356^{-4}}$, and computational time is found as $3.5615 msec$. The given test is conducted on an Intel i7, 8GB computer using MATLAB environment.

Case 2: In this case, 38 bus system is employed to assess the computational performance of the LAV based and WLS based estimators. As seen in Table 5.3, the

proposed partial linearization of the measurement function improves the computational time. As the system size expands, the difference becomes more significant. Although WLS is the fastest compared to the LAV based estimators, an additional pre-process, namely bad data detection is required to obtain accurate results. Considering the inserted pseudo injection measurements are unreliable, WLS without bad data detection estimates the states with bias. On the other hand, since the nature of the LAV based estimation relies on selecting the minimum number of measurements satisfying the least absolute values of error, LAV based estimation automatically rejects bad/biased data. 500 Monte-Carlo simulations are executed on an Intel i7, 8GB computer to obtain unbiased results.

Table 5.3 Computational performance results for 38 bus system

Type of Estimation	Computational Time
Original LAV Estimation	$250msec$
Proposed LAV Estimation	$238msec$
WLS Estimation	$68msec$

The aim of using state estimation in this study is to find the most probable system state based on real-time measurements and to validate the actions. As seen in the results, the computation time for the 38 bus test system is in the order of hundreds of milliseconds. Although this performance might not be sufficient for conventional real-time monitoring and control problems, it is acceptable for validation of the restoration process.

Case 3: In order to validate the selection of estimation method, the 3-bus sample system shown in Figure 5.3. is utilized. The accuracy of LAV estimation and WLS estimation for the given system is compared with and without biased data. The test is conducted on an Intel i7, 8GB computer.

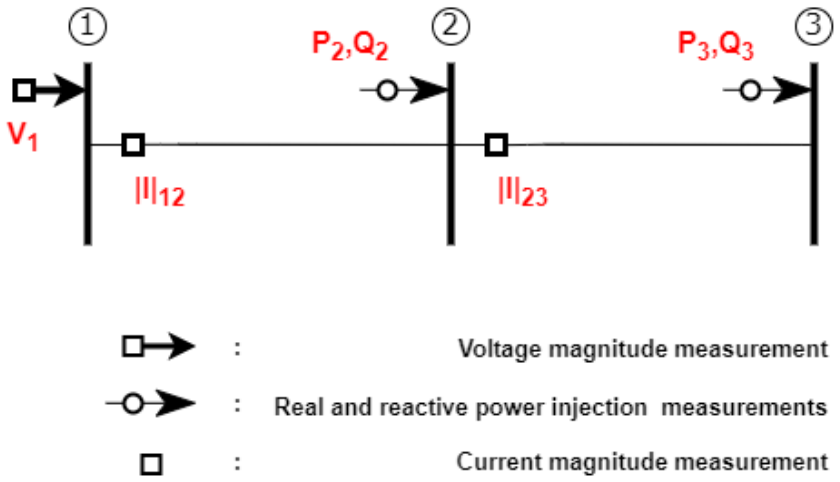

Figure 5.3. Sample 3-bus system with a measurement configuration

In Table 5.4, the MSE of the estimated states for two estimators is given with and without bad data. As seen in the table, without bad data, the WLS estimator is superior to the LAV based estimator since WLS aims to minimize the MSE. However, when a bad (biased) data is inserted to reflect the effect of unreliable pseudo measurements, the result of WLS is highly biased whereas the LAV estimator is robust against the biased data.

Table 5.4 Estimation results for different measurement sets

Type of Estimator	*MSE without bad data*	*MSE with bad data*
WLS	1.065×10^{-10}	0.0043
LAV	3.65×10^{-10}	3.65×10^{-10}

The performance of the estimator under biased data is crucial considering the lack of measurements and the unreliable nature of pseudo measurements in the distribution system.

In Figure 5.4, the collected measurements, the actual (true) values of the measurements, the estimated measurements by LAV and WLS estimators are given. As seen in the figure, the real power injection of bus-2 is manipulated to assess the robustness of the estimator. While real power injection measurement, P_2, and current magnitude measurement, I_{12}, are significantly biased using WLS estimation, the estimated measurements by LAV are completely unbiased. This case shows that while LAV estimation provides automatic rejection of the bad data, unreliable pseudo measurement, an additional bad data analysis is required in WLS estimation to obtain unbiased results with low redundancy as in the distribution system.

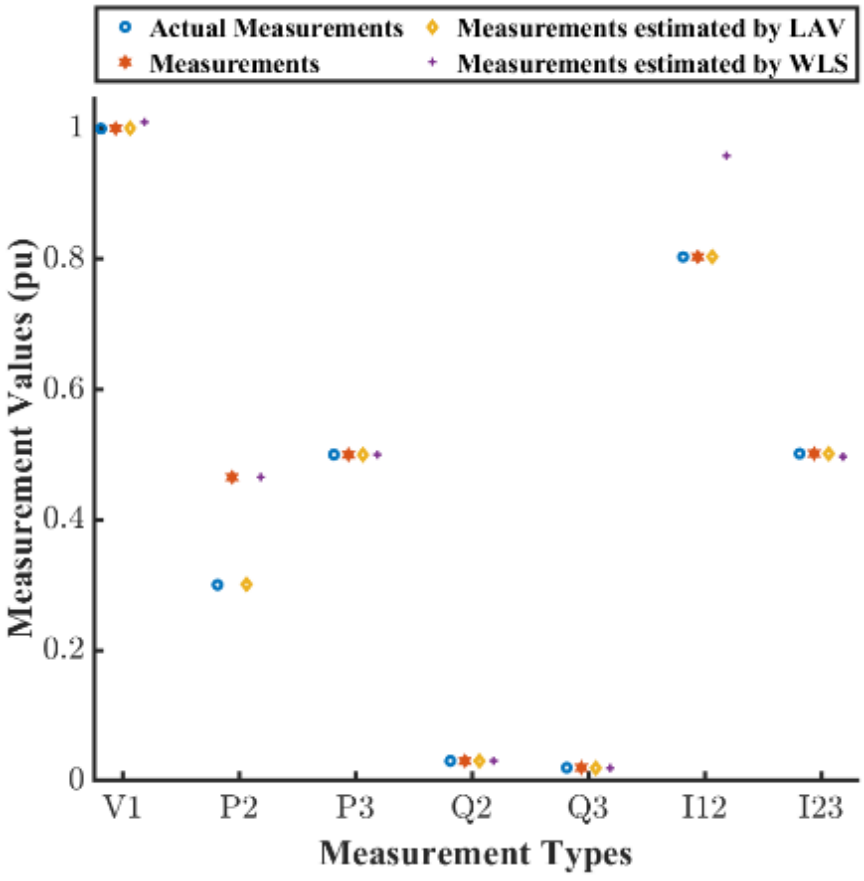

Figure 5.4. Comparison of WLS and LAV estimation under biased measurements

Case 4: In this case, a 12-bus system is employed to reveal the accuracy of the estimators. %1 Gaussian error is added to the measurement set to make the accuracy results noticeable. In Table 5.5, the metrics used to evaluate the accuracy are MSE and MAPE. While the error of the proposed LAV estimator is comparable with the original LAV estimator, the accuracy of the WLS estimation has the best performance comparing to LAV based estimators. However, in this application the accuracy under biased data is critical considering the unreliable pseudo injection measurements. Therefore, as validated in Case-3, the LAV based estimation which is robust against bad data is utilized. The test is conducted on an Intel i7, 8GB computer.

Table 5.5 State estimation results for 12 bus system

Type of Estimation	*MSE*	*MAPE*
Original LAV Estimation	3.122×10^{-8}	0.0574
Proposed LAV Estimation	4.525×10^{-8}	0.0582
WLS Estimation	1.186×10^{-8}	0.0552

Case 5: The proposed estimator is also utilized in a 600 bus system which is a subpart of a real-life distribution system. The computational time of the process in the 600 Bus system is **2.67** seconds. To test the computational time, 2xIntel(R) Xeon(R) CPU E5-2650 v4 @ 2.20GHz with 64GB RAM hardware setup is used. 5 Monte-Carlo simulations are run, and their average is given as a result.

5.3 Chapter Summary

In this chapter, the proposed methods are validated. Firstly, the effectiveness of the partitioning method is validated in different cases. The partitioning of the 8477 bus

system in under a minute shows that the partitioning method can be utilized in a real-time online decision process. Furthermore, the comparison of MCB only and RDE followed by MCB shows that the computational performance of identification of the system can be significantly improved. In the corresponding graph, it is shown that MCB only method fails in the systems with around ten thousand. Considering the size of the distribution systems can be a few tens of thousands, and they expand continuously, the proposed partitioning method is crucial to analyze the systems in a fast manner.

The performance of the situational awareness tool is also validated in this chapter. The reasoning of the LAV based estimation is selected as distribution system estimation is justified. The results related to the performance improvement of the estimator show that the gain in the computational performance is promising while the accuracy is comparable. The robustness and accuracy of the LAV based estimation are validated using the sample system to provide the audience better understanding. As a result, the tests show that both the FBPF and LAV estimator are efficient and accurate enough to be utilized in the restoration to improve the situational awareness.

CHAPTER 6

CONCLUSION

In this thesis, the overall performance of the distribution system restoration procedure is improved. The aim of the given work can be divided into two where the novel partitioning algorithm improves the computational performance of the restoration decision process; the situational awareness monitors the power system and predicts the possible infeasible actions to be realized.

The partitioning algorithm is employed to detect the ring and radial structures in the distribution system topology so that restoration strategy can be obtained for the ring/radial structures separately. In addition to that, the situational awareness tool is developed to monitor the power system and predict the possible infeasible actions to be realized. The LAV based three-phase state estimator is proposed in this study to monitor the system in real-time using the measurements gathered from the energized part of the system. Furthermore, the performance of the estimator is improved by partial linearization of the measurement function.

The efficiency of the partitioning method is validated by comparing the computational time of the restoration decision process with/without utilizing the proposed DRS method. Furthermore, in the thesis, it is also shown that utilizing the DRS method increases the performance of identification of each ring since the graph based method is employed only to ring structured part instead of the whole system.

The robustness, accuracy and time performances of the conventional LAV based estimation, the LAV based estimation with the proposed measurement function, and WLS based estimation are presented to validate the superiority of the proposed estimation method. The sequential operation of the estimator and the flow analysis ensures that the energized part of the system is monitored in real-time using reliable

measurements, and the given action set can be realized in the whole system by power flow analysis using load/generation forecasts and profiles of the un-energized part.

To sum up, the partitioning method improves the performance of the system analysis to be utilized in the online decision support mechanism for distribution system restoration. The partitioning method makes the online decision support mechanism for the restoration of large-sized distribution systems possible. Moreover, the partitioning method is capable of analyzing large-sized systems where graph based methods may fail to converge in a reasonable time. The test results show that both the FBPF and developed LAV estimator are efficient and accurate enough to be utilized in the restoration to improve the situational awareness. Considering the heuristic and rule-based restoration procedures available in the literature, the proposed restoration methodology optimizes the restoration strategy considering electrical constraints

As future work, PMUs can also be included. PMUs are not considered in this study since PMUs are not commonly used distribution systems. However, in the presence of those measurements, the proposed method can be used without loss of generality. Moreover, the estimator can be constructed using the sparse data structure. The computational performance of the estimator is expected to increase significantly in sparse structure considering the sparsity ratio of the utilized matrices.

REFERENCES

[1] T. Nagata, S. Hatakeyama, M. Yasuoka, and H. Sasaki, “An efficient method for power distribution system restoration based on mathematical programming and operation strategy,” in *PowerCon 2000 - 2000 International Conference on Power System Technology, Proceedings*, 2000, vol. 3, pp. 1545–1550, doi: 10.1109/ICPST.2000.898201.

[2] Y. Liu, R. Fan, and V. Terzija, “Power system restoration: a literature review from 2006 to 2016,” *J. Mod. Power Syst. Clean Energy*, vol. 4, no. 3, pp. 332–341, Jul. 2016, doi: 10.1007/s40565-016-0219-2.

[3] G. Patsakis, D. Rajan, I. Aravena, J. Rios, and S. Oren, “Optimal black start allocation for power system restoration,” *IEEE Trans. Power Syst.*, vol. 33, no. 6, pp. 6766–6776, Nov. 2018, doi: 10.1109/TPWRS.2018.2839610.

[4] J. J. Ancona, “A Framework For Power System Restoration Following a Major Power Failure,” *IEEE Trans. Power Syst.*, vol. 10, no. 3, pp. 1480–1485, 1995, doi: 10.1109/59.466500.

[5] M. T. Bina and A. Kashefi, “Three-phase unbalance of distribution systems: Complementary analysis and experimental case study,” *Int. J. Electr. Power Energy Syst.*, vol. 33, no. 4, pp. 817–826, May 2011, doi: 10.1016/j.ijepes.2010.12.003.

[6] D. Della Giustina, M. Pau, P. A. Pegoraro, F. Ponci, and S. Sulis, “Electrical distribution system state estimation: Measurement issues and challenges,” *IEEE Instrum. Meas. Mag.*, vol. 17, no. 6, pp. 36–42, Dec. 2014, doi: 10.1109/MIM.2014.6968929.

[7] E. Manitsas, R. Singh, B. Pal, and G. Strbac, “Modelling of pseudo-measurements for distribution system state estimation,” in *IET Seminar Digest*, 2008, vol. 2008, no. 12380, doi: 10.1049/ic:20080447.

[8] Y. Sarkale, S. Nozhati, E. K. P. Chong, and B. R. Ellingwood, “Decision automation for electric power network recovery,” *arXiv*. 2019.

[9] E. A. Gol, B. G. Erkal, and M. Göl, “A Novel MDP Based Decision Support Framework to Restore Earthquake Damaged Distribution Systems,” Sep. 2019, doi: 10.1109/ISGTEurope.2019.8905675.

[10] O. Y. Arpali, U. C. Yilmaz, E. A. Gol, B. G. Erkal, and M. Gol, “MDP based decision support for earthquake damaged distribution system restoration,” in *IEEE Power and Energy Society General Meeting*, Aug. 2020, vol. 2020-August, doi: 10.1109/PESGM41954.2020.9281815.

[11] G. Cavraro and V. Kekatos, “Graph Algorithms for Topology Identification Using Power Grid Probing,” *IEEE Control Syst. Lett.*, vol. 2, no. 4, pp. 689–694, 2018, doi: 10.1109/LCSYS.2018.2846801.

[12] S. Park, D. Deka, and M. Chcrtkov, “Exact topology and parameter estimation in distribution grids with minimal observability,” Aug. 2018, doi: 10.23919/PSCC.2018.8442881.

[13] S. Bolognani, N. Bof, D. Michelotti, R. Muraro, and L. Schenato, “Identification of power distribution network topology via voltage correlation analysis,” in *Proceedings of the IEEE Conference on Decision and Control*, 2013, pp. 1659–1664, doi: 10.1109/CDC.2013.6760120.

[14] D. Deka, S. Talukdar, M. Chertkov, and M. Salapaka, “Topology Estimation in Bulk Power Grids: Guarantees on Exact Recovery,” Jul. 2017, Accessed: Jun. 02, 2021. [Online]. Available: http://arxiv.org/abs/1707.01596.

[15] D. Deka, S. Backhaus, and M. Chertkov, “Learning topology of the power distribution grid with and without missing data,” in *2016 European Control Conference, ECC 2016*, 2016, pp. 313–320, doi: 10.1109/ECC.2016.7810304.

[16] J. J. Grainger and W. D. Stevenson, “Power System Analysis,” 1994. .

[17] B. Hayes and M. Prodanović, “State estimation techniques for electric power distribution systems,” in *Proceedings - UKSim-AMSS 8th European Modelling Symposium on Computer Modelling and Simulation, EMS 2014*, 2014, pp. 303–308, doi: 10.1109/EMS.2014.76.

[18] H. Rudnick and M. Munoz, “Influence of modeling in load flow analysis of three phase distribution systems,” in *Proceedings of the 1990 IEEE Colloquium in South America, COLLOQ 1990*, 1990, pp. 173–176, doi: 10.1109/COLLOQ.1990.152825.

[19] M. E. Baran and A. W. Kelley, “State Estimation for Real-Time Monitoring of Distribution Systems,” *IEEE Trans. Power Syst.*, vol. 9, no. 3, pp. 1601–1609, 1994, doi: 10.1109/59.336098.

[20] P. Chusovitin, I. Polyakov, and A. Pazderin, “Three-phase state estimation model for distribution grids,” Jan. 2017, doi: 10.1109/ICSEE.2016.7806063.

[21] R. James Ranjith Kumar and A. Jain, “Load flow methods in distribution systems with dispersed generations: A brief review,” Apr. 2015, doi: 10.1109/ICPDEN.2015.7084498.

[22] S. Chatterjee and S. Mandal, “A novel comparison of gauss-seidel and newton- raphson methods for load flow analysis,” in *2017 International Conference on Power and Embedded Drive Control (ICPEDC)*, 2017, pp. 1–7, doi: 10.1109/ICPEDC.2017.8081050.

[23] M. S. Srinivas, “Distribution load flows: A brief review,” in *2000 IEEE Power Engineering Society, Conference Proceedings*, 2000, vol. 2, pp. 942–945, doi: 10.1109/PESW.2000.850058.

[24] W. H. Kersting, *Distribution System Modeling and Analysis*. Taylor \& Francis, CRC Press, 2017.

[25] R. Berg, E. S. Hawkins, and W. W. Pleines, “Mechanized Calculation of Unbalanced Load Flow on Radial Distribution Circuits,” *IEEE Trans. Power*

Appar. Syst., vol. PAS-86, no. 4, pp. 415–421, 1967, doi: 10.1109/TPAS.1967.291849.

[26] J. H. Teng and C. Y. Chang, “A novel and fast three-phase load flow for unbalanced radial distribution systems,” *IEEE Trans. Power Syst.*, vol. 17, no. 4, pp. 1238–1244, 2002, doi: 10.1109/TPWRS.2002.805012.

[27] B. Muruganantham, R. Gnanadass, and N. P. Padhy, “Performance analysis and comparison of load flow methods in a practical distribution system,” Feb. 2017, doi: 10.1109/NPSC.2016.7858848.

[28] A. Majumdar and B. C. Pal, “A three-phase state estimation in unbalanced distribution networks with switch modelling,” in *2016 IEEE 1st International Conference on Control, Measurement and Instrumentation, CMI 2016*, Feb. 2016, pp. 474–478, doi: 10.1109/CMI.2016.7413793.

[29] F. Ahmad, A. Rasool, E. Ozsoy, R. Sekar, A. Sabanovic, and M. Elitaş, “Distribution system state estimation-A step towards smart grid,” *Renewable and Sustainable Energy Reviews*, vol. 81. Elsevier Ltd, pp. 2659–2671, Jan. 01, 2018, doi: 10.1016/j.rser.2017.06.071.

[30] A. Abur and A. G. Exposito, *Power System State Estimation: Theory and Implementation*. 2004.

[31] F. C. Schweppe and J. Wildes, “Power System Static-State Estimation, Part I: Exact Model,” *IEEE Trans. Power Appar. Syst.*, vol. PAS-89, no. 1, pp. 120–125, 1970, doi: 10.1109/TPAS.1970.292678.

[32] F. C. Schweppe and D. B. Rom, “Power System Static-State Estimation, Part II: Approximate Model,” *IEEE Trans. Power Appar. Syst.*, vol. PAS-89, no. 1, pp. 125–130, 1970, doi: 10.1109/TPAS.1970.292679.

[33] F. C. Schweppe, “Power System Static-State Estimation, Part III: Implementation,” *IEEE Trans. Power Appar. Syst.*, vol. PAS-89, no. 1, pp. 130–135, 1970, doi: 10.1109/TPAS.1970.292680.

[34] N. J. Higham, “Cholesky factorization,” in *Wiley Interdisciplinary Reviews: Computational Statistics*, Sep. 2009, vol. 1, no. 2, pp. 251–254, doi: 10.1002/wics.18.

[35] M. Farajollahi, A. Shahsavari, and H. Mohsenian-Rad, “Topology Identification in Distribution Systems Using Line Current Sensors: An MILP Approach,” *IEEE Trans. Smart Grid*, vol. 11, no. 2, pp. 1159–1170, Mar. 2020, doi: 10.1109/TSG.2019.2933006.

[36] X. Zhang, Y. Li, C. Yang, S. Wang, W. Xie, and P. Ling, “Topology Analysis of Distribution Network Based on μPMU and SCADA,” in *2018 International Conference on Power System Technology, POWERCON 2018 - Proceedings*, Jan. 2019, pp. 3427–3433, doi: 10.1109/POWERCON.2018.8602298.

[37] D. Deka, M. Chertkov, and S. Backhaus, “Topology Estimation Using Graphical Models in Multi-Phase Power Distribution Grids,” *IEEE Trans. Power Syst.*, vol. 35, no. 3, pp. 1663–1673, May 2020, doi: 10.1109/TPWRS.2019.2897004.

[38] E. Caro and A. J. Conejo, “State estimation via mathematical programming: A comparison of different estimation algorithms,” *IET Gener. Transm. Distrib.*, vol. 6, no. 6, pp. 545–553, Jun. 2012, doi: 10.1049/iet-gtd.2011.0663.

[39] X. T. Jiang, B. Fardanesh, D. Maragal, G. Stefopoulos, J. H. Chow, and M. Razanousky, “Improving performance of the non-iterative direct state estimation method,” 2014, doi: 10.1109/PECI.2014.6804562.

[40] X. T. Jiang, J. H. Chow, B. Fardanesh, D. Maragal, G. Stefopoulos, and M. Razanousky, “Power system state estimation using a direct non-iterative method,” *Int. J. Electr. Power Energy Syst.*, vol. 73, pp. 361–368, Dec. 2015, doi: 10.1016/j.ijepes.2015.05.025.

APPENDICES

A. The Formulation of Elements of Jacobian Matrix

$$
\begin{aligned}
\frac{\partial {P_i}^A}{\partial {V_i}^A} = & \sum_{j \in N_i} V_j^A \left(G_{ij}^{A,A} + B_{ij}^{A,A} \left(\theta_A^i - \theta_A^j \right) \right) \\
& + \sum_{j \in N_i} V_j^B \left(G_{ij}^{A,B} \left(cos\left(\frac{2\pi}{3}\right) - sin\left(\frac{2\pi}{3}\right) \right. \right. \\
& \left. \cdot \left(\theta_A^i - \theta_B^j + \frac{2\pi}{3} \right) \right) \\
& + B_{ij}^{A,B} \left(cos\left(\frac{2\pi}{3}\right) \cdot \left(\theta_A^i - \theta_B^j + \frac{2\pi}{3} \right) + sin\left(\frac{2\pi}{3}\right) \right) \Bigg) \\
& + \sum_{j \in N_i} V_j^C \left(G_{ij}^{A,C} \left(cos\left(\frac{2\pi}{3}\right) + sin\left(\frac{2\pi}{3}\right) \right. \right. \\
& \left. \cdot \left(\theta_A^i - \theta_C^j + \frac{2\pi}{3} \right) \right) \\
& + B_{ij}^{A,C} \left(cos\left(\frac{2\pi}{3}\right) \cdot \left(\theta_A^i - \theta_C^j + \frac{2\pi}{3} \right) - sin\left(\frac{2\pi}{3}\right) \right) \Bigg) \\
& + 2 \cdot V_i^A \left(G_{ii}^{AA} \right) \\
& + V_i^B \left(G_{ii}^{A,B} \left(cos\left(\frac{2\pi}{3}\right) - sin\left(\frac{2\pi}{3}\right) \cdot \left(\theta_A^i - \theta_B^j + \frac{2\pi}{3} \right) \right) \right. \\
& + B_{ii}^{A,B} \left(cos\left(\frac{2\pi}{3}\right) \cdot \left(\theta_A^i - \theta_B^j + \frac{2\pi}{3} \right) + sin\left(\frac{2\pi}{3}\right) \right) \Bigg) \\
& + V_i^C \left(G_{ii}^{A,C} \left(cos\left(\frac{2\pi}{3}\right) + sin\left(\frac{2\pi}{3}\right) \cdot \left(\theta_A^i - \theta_C^j + \frac{2\pi}{3} \right) \right) \right. \\
& + B_{ii}^{A,C} \left(cos\left(\frac{2\pi}{3}\right) \cdot \left(\theta_A^i - \theta_C^j + \frac{2\pi}{3} \right) - sin\left(\frac{2\pi}{3}\right) \right) \Bigg)
\end{aligned}
\tag{A.1}
$$

$$
\begin{aligned}
\frac{\partial Q_i{}^A}{\partial \theta_i{}^A} = & \sum_{j \in N_i} V_i^A V_j^A \left(G_{ij}^{A,A} + B_{ij}^{A,A} \left(\theta_A^i - \theta_A^j \right) \right) \\
& + \sum_{j \in N_i} V_i^A V_j^l \left(G_{ij}^{A,B} \left(cos\left(\frac{2\pi}{3}\right) - sin\left(\frac{2\pi}{3}\right) \right. \right. \\
& \left. \cdot \left(\theta_A^i - \theta_B^j + \frac{2\pi}{3} \right) \right) \\
& \left. + B_{ij}^{A,B} \left(cos\left(\frac{2\pi}{3}\right) \cdot \left(\theta_A^i - \theta_B^j + \frac{2\pi}{3} \right) + sin\left(\frac{2\pi}{3}\right) \right) \right) \\
& + \sum_{j \in N_i} V_i^A V_j^C \left(G_{ij}^{A,C} \left(cos\left(\frac{2\pi}{3}\right) + sin\left(\frac{2\pi}{3}\right) \right. \right. \\
& \left. \cdot \left(\theta_A^i - \theta_C^j + \frac{2\pi}{3} \right) \right) \\
& \left. + B_{ij}^{A,C} \left(cos\left(\frac{2\pi}{3}\right) \cdot \left(\theta_A^i - \theta_C^j + \frac{2\pi}{3} \right) - sin\left(\frac{2\pi}{3}\right) \right) \right) + \\
& \cdot V_i^A V_i^B \left(G_{ii}^{A,B} \left(cos\left(\frac{2\pi}{3}\right) - sin\left(\frac{2\pi}{3}\right) \right. \right. \\
& \left. \cdot \left(\theta_A^i - \theta_B^j + \frac{2\pi}{3} \right) \right) \\
& \left. + B_{ii}^{AA} \left(cos\left(\frac{2\pi}{3}\right) \cdot \left(\theta_A^i - \theta_B^j + \frac{2\pi}{3} \right) + sin\left(\frac{2\pi}{3}\right) \right) \right) \\
& + V_i^A V_i^C \left(G_{ii}^{A,C} \left(cos\left(\frac{2\pi}{3}\right) + sin\left(\frac{2\pi}{3}\right) \right. \right. \\
& \left. \cdot \left(\theta_A^i - \theta_C^j + \frac{2\pi}{3} \right) \right) \\
& \left. + B_{ii}^{A,C} \left(cos\left(\frac{2\pi}{3}\right) \cdot \left(\theta_A^i - \theta_C^j + \frac{2\pi}{3} \right) - sin\left(\frac{2\pi}{3}\right) \right) \right)
\end{aligned}
\tag{A.2}
$$

$$
\begin{aligned}
\frac{\partial {Q_i}^A}{\partial {V_i}^A} = & \sum_{j \in N_i} V_j^A \left(G_{ij}^{A,A} \left(\theta_A^i - \theta_A^j \right) - B_{ij}^{A,A} \right) \\
& + \sum_{j \in N_i} V_j^l \left(G_{ij}^{A,B} \left(cos\left(\frac{2\pi}{3}\right) \cdot \left(\theta_A^i - \theta_B^j + \frac{2\pi}{3} \right) \right. \right. \\
& \left. + sin\left(\frac{2\pi}{3}\right) \right) \\
& \left. - B_{ij}^{A,B} \left(cos\left(\frac{2\pi}{3}\right) - sin\left(\frac{2\pi}{3}\right) \cdot \left(\theta_A^i - \theta_B^j + \frac{2\pi}{3} \right) \right) \right) \\
& + \sum_{j \in N_i} V_j^C \left(G_{ij}^{A,C} \left(cos\left(\frac{2\pi}{3}\right) \cdot \left(\theta_A^i - \theta_C^j + \frac{2\pi}{3} \right) \right. \right. \\
& \left. - sin\left(\frac{2\pi}{3}\right) \right) \\
& \left. - B_{ij}^{A,C} \left(cos\left(\frac{2\pi}{3}\right) + sin\left(\frac{2\pi}{3}\right) \cdot \left(\theta_A^i - \theta_C^j + \frac{2\pi}{3} \right) \right) \right) \\
& + 2 \cdot V_i^A \left(-B_{ii}^{AA} \right) \\
& + V_i^B \left(G_{ii}^{A,B} \left(cos\left(\frac{2\pi}{3}\right) \cdot \left(\theta_A^i - \theta_B^j + \frac{2\pi}{3} \right) + sin\left(\frac{2\pi}{3}\right) \right) \right. \\
& \left. - B_{ii}^{A,B} \left(cos\left(\frac{2\pi}{3}\right) - sin\left(\frac{2\pi}{3}\right) \cdot \left(\theta_A^i - \theta_B^j + \frac{2\pi}{3} \right) \right) \right) \\
& + V_i^C \left(G_{ii}^{A,C} \left(cos\left(\frac{2\pi}{3}\right) \cdot \left(\theta_A^i - \theta_C^j + \frac{2\pi}{3} \right) - sin\left(\frac{2\pi}{3}\right) \right) \right. \\
& \left. - B_{ii}^{A,C} \left(cos\left(\frac{2\pi}{3}\right) + sin\left(\frac{2\pi}{3}\right) \cdot \left(\theta_A^i - \theta_C^j + \frac{2\pi}{3} \right) \right) \right)
\end{aligned}
\tag{A.3}
$$

$$
\begin{aligned}
\frac{\partial P_i{}^A}{\partial \theta_i{}^A} = & \sum_{j \in N_i} V_i^A V_j^A \left(-G_{ij}^{A,A}\left(\theta_A^i - \theta_A^j\right) + B_{ij}^{A,A}\right) \\
& + \sum_{j \in N_i} V_i^A V_j^l \left(-G_{ij}^{A,B}\left(cos\left(\frac{2\pi}{3}\right) \cdot \left(\theta_A^i - \theta_B^j + \frac{2\pi}{3}\right)\right.\right. \\
& \left. + sin\left(\frac{2\pi}{3}\right)\right) \\
& \left. + B_{ij}^{A,B}\left(cos\left(\frac{2\pi}{3}\right) - sin\left(\frac{2\pi}{3}\right) \cdot \left(\theta_A^i - \theta_B^j + \frac{2\pi}{3}\right)\right)\right) \\
& + \sum_{j \in N_i} V_i^A V_j^C \left(-G_{ij}^{A,C}\left(cos\left(\frac{2\pi}{3}\right) \cdot \left(\theta_A^i - \theta_C^j + \frac{2\pi}{3}\right)\right.\right. \\
& \left. - sin\left(\frac{2\pi}{3}\right)\right) \\
& \left. + B_{ij}^{A,C}\left(cos\left(\frac{2\pi}{3}\right) + sin\left(\frac{2\pi}{3}\right) \cdot \left(\theta_A^i - \theta_C^j + \frac{2\pi}{3}\right)\right)\right) + \\
& \cdot V_i^A V_i^B \left(-G_{ii}^{A,B}\left(cos\left(\frac{2\pi}{3}\right) \cdot \left(\theta_A^i - \theta_B^j + \frac{2\pi}{3}\right)\right.\right. \\
& \left. + sin\left(\frac{2\pi}{3}\right)\right) \\
& \left. + B_{ii}^{AA}\left(cos\left(\frac{2\pi}{3}\right) - sin\left(\frac{2\pi}{3}\right) \cdot \left(\theta_A^i - \theta_B^j + \frac{2\pi}{3}\right)\right)\right) \\
& + V_i^A V_i^C \left(-G_{ii}^{A,C}\left(cos\left(\frac{2\pi}{3}\right) \cdot \left(\theta_A^i - \theta_C^j + \frac{2\pi}{3}\right)\right.\right. \\
& \left. - sin\left(\frac{2\pi}{3}\right)\right) \\
& \left. + B_{ii}^{A,C}\left(cos\left(\frac{2\pi}{3}\right) + sin\left(\frac{2\pi}{3}\right) \cdot \left(\theta_A^i - \theta_C^j + \frac{2\pi}{3}\right)\right)\right)
\end{aligned}
\tag{A.4}
$$

B. Input Files for The Distribution System State Estimation

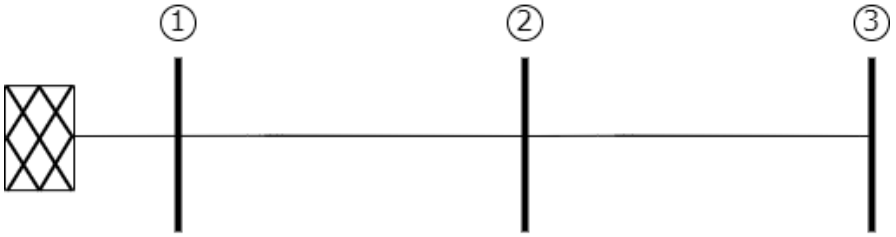

Figure B.1. Sample 3 bus system

```
                                                    100.0
BUS DATA FOLLOWS                 V_A     V_B     V_C    delA    delB    delC
   1                 0000   3 1.0600  1.0600  1.0600    0.00    0.00    0.00
   2                 0000   0 1.0450  1.0450  1.0450   -4.98   -4.98   -4.98
   3                 0000   0 1.0100  1.0100  1.0100  -12.72  -12.72  -12.72
-999
BRANCH DATA FOLLOWS            R_AA       R_AB      R_AC      R_BB      R_BA
   1    2  0000 0 0     0.0470     0.02350     0.0235     0.0470     0.0235
   2    3  0000 0 0     0.0470     0.02350     0.0235     0.0470     0.0235
-999
LOSS ZONES FOLLOWS
-99
INTERCHANGE DATA FOLLOWS
-9
TIE LINES FOLLOWS
-999
END OF DATA
```

Figure B.2. CDF file structure of a sample distribution system

```
1
1     19918.58 0.001 0
1
1     19918.58 0.001 0
1
1     19918.58 0.001 0
2
2    -10015.4  1 1.0450
3    -16669.1  0 1.0100
2
2    -10015.4  1 1.0450
3    -16669.1  0 1.0100
2
2    -10015.4  1 1.0450
3    -16669.1  0 1.0100
2
2    -1018.79  0 1.0450
3    -670.166  0 1.0100
2
2    -1018.79  0 1.0450
3    -670.166  0 1.0100
2
2    -1018.79  0 1.0450
3    -670.166  0 1.0100
2
1    2  1344.37 0
2    3  839.595 0
2
1    2  1344.37 0
2    3  839.595 0
2
1    2  1344.37 0
2    3  839.595 0
```

Figure B.3. Measurement file of a sample distribution system